Course in 3 lectures on

Superfluidity in Ultracold Fermi Gases

Francesca Maria Marchetti
Rudolf Peierls Centre for Theoretical Physics
University of Oxford

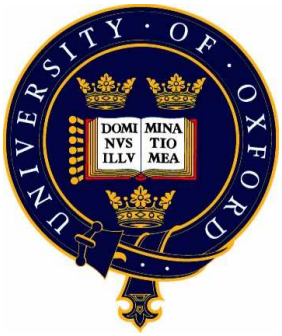

Physics by the Lake

Ambleside, September 2007

Abstract

The search for novel phases of quantum coherent matter has been one of the main driving forces in condensed matter physics for many years. The unprecedented experimental sophistication reached recently in ultracold atomic gases has opened new and exciting perspectives in this search. The ability to externally manipulate the interatomic interaction, the capacity to embed atomic clouds in optical lattices or confine them in low dimensions, as well as the possibility to prepare mixtures of atoms with different statistics and/or populations, is presenting an opportunity to realise and explore novel correlated phases of matter. During the lectures I will focus mainly on aspects of condensation and superfluidity phenomena in fermionic systems. Theoretical elements will be discussed together with recent experimental realisations.

Contents

Chapter 1

Lecture I: Weakly interacting Fermi gases

After the first realisation of Bose-Einstein condensation for the bosonic species [2, 8], remarkable effort has been devoted to realise and explore degenerate ultracold Fermi gases. One of the main interests, aside the realisation of a the textbook example of a non-interacting ideal Fermi gas (see Secs. 1.1 and 1.1.2), has been the reach of the necessary conditions to observe a transition to a superfluid state of fermionic pairs, similarly to the Bardeen-Cooper-Schrieffer (BCS) transition (see Sec. 1.3) which happens for ordinary low temperatures superconductors. Such experiments will be discussed during Lecture II (see Sec. 2.4).

1.1 The ideal Fermi gas

Although the main experimental challenge in the study of degenerate ultracold Fermi gases has been the realisation of a superfluid phase, even an ideal non-interacting Fermi gas can provide useful information about the properties of the Fermi statistics, as we will see in Sec. 1.1.2.

At very low densities or high temperatures, a gas of bosons and a gas of fermions behave classically. The quantum behaviour in both cases is governed by the *phase-space density* (everywhere in these lecture notes we will fix $\hbar = 1$),

$$\rho = n\lambda_T^3 \qquad\qquad \lambda_T = \left(\frac{2\pi}{mk_BT}\right)^{1/2}, \tag{1.1}$$

which is a measure of the average distance between the atoms $n^{-1/3}$ compared to the thermal de Broglie wavelength λ_T. Quantum behaviour emerges when ρ increases to values of the order of unity. In the case of bosons, the transition to a Bose-Einstein condensate happens for $\rho = \zeta(3/2) \simeq 2.612$ [27]. In the case of fermions, when ρ reaches a value of the order of 1, fermions tend to fill all the available low energy states, with one particle only per state, up to the Fermi energy.

Therefore, whether we are considering the case of N identical fermions either in a box of volume V (with density $n = N/V$) or in a three-dimensional harmonic trap, the zero temperature ground state of the system is characterised by all

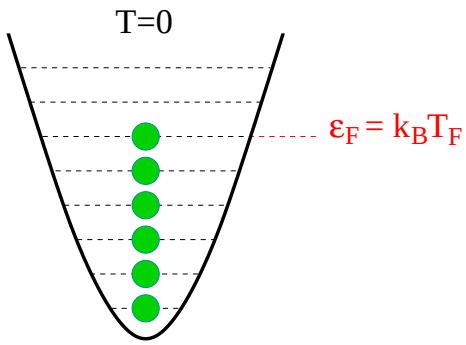

Figure 1.1: Sketch of the definition of the Fermi temperature for a Fermi gas in a harmonic trap.

states with energy less than the Fermi energy being occupied, while those with higher energy being empty. The Fermi energy is therefore defined as

$$N = G(\varepsilon_F) \,, \tag{1.2}$$

where $G(\epsilon)$ is the number of states with energy less than ϵ.

Problem: Evaluate $G(\epsilon)$ for N particles in a box of volume V and for a three-dimensional harmonic potential $V(\mathbf{r}) = m(\omega_1^2 x^2 + \omega_2^2 y^2 + \omega_3^2 z^2)/2$:

$$G(\epsilon) = \frac{V(2m\epsilon)^{3/2}}{6\pi^2} \qquad \text{box} \tag{1.3}$$

$$G(\epsilon) = \frac{\epsilon^3}{6\bar{\omega}^3} \qquad \text{3D harmonic trap} \,, \tag{1.4}$$

where $\bar{\omega} = (\omega_1\omega_2\omega_3)^{1/3}$.

Answer: For a particle in a box one has

$$G(\epsilon) = \sum_{\mathbf{k}}^{\epsilon_{\mathbf{k}} \leq \epsilon} = V \int \frac{d\mathbf{k}}{(2\pi)^3} \theta(\epsilon - \epsilon_{\mathbf{k}}) \,,$$

where $\epsilon_{\mathbf{k}} = \mathbf{k}^2/2m$. For an harmonic oscillator potential, one has the discrete energy levels $\epsilon = \sum_i \epsilon_i = \sum_i (n_i + 1/2)\omega_i$, with $i = 1, 2, 3$. For energies ϵ large compared with ω_i, one can neglect the zero point motion and approximate n_i as continuous variables. Then $G(\epsilon)$ is given by a three-dimensional integral limited on the plane by the constraint $\epsilon = \epsilon_1 + \epsilon_2 + \epsilon_3$:

$$G(\epsilon) = \frac{1}{\bar{\omega}^3} \int_0^{\epsilon} d\epsilon_1 \int_0^{\epsilon-\epsilon_1} d\epsilon_2 \int_0^{\epsilon-\epsilon_1-\epsilon_2} d\epsilon_3 \,.$$

Using the expressions (1.3) and (1.4), one obtains the following expressions for the Fermi energy ε_F and the Fermi temperature $k_B T_F = \varepsilon_F$, i.e. the temper-

ature below which quantum behaviour of fermions starts emerging (see Fig 1.1):

$$k_B T_F = \varepsilon_F = \frac{(6\pi^2)^{2/3}}{2}\frac{n^{2/3}}{m} \simeq 7.6\frac{n^{2/3}}{m} \tag{1.5}$$

$$k_B T_F = \varepsilon_F = \bar{\omega}(6N)^{1/3} \simeq 1.82\bar{\omega}N^{1/3} \, . \tag{1.6}$$

Problem: Derive the expressions for the transition temperature to a BEC for N identical bosons respectively in a box of volume V and in a three-dimensional harmonic potential:

$$k_B T_{\rm BEC} = \frac{2\pi}{[\zeta(3/2)]^{2/3}}\frac{n^{2/3}}{m} \simeq 3.3\frac{n^{2/3}}{m} \tag{1.7}$$

$$k_B T_{\rm BEC} = \frac{1}{[\zeta(3)]^{1/3}}\bar{\omega}N^{1/3} \simeq 0.94\bar{\omega}N^{1/3} \, . \tag{1.8}$$

The Fermi energy has the same dependence on the system parameters (i.e. the density and mass of the gas in case of N particles in a box and the number of atoms and the oscillator frequency $\bar{\omega}$ if the gas is trapped) as the BEC critical temperature. This is not surprising as in both cases quantum degeneracy emerges when $\rho \gtrsim 1$. [1] However, note that, while for a Bose-Einstein condensate $T_{\rm BEC}$ marks the value of the temperature at which a phase transition happens, T_F represent the temperature at which the *crossover* from the classical to the quantum regime happens.

The total energy of an ideal Fermi gas can be evaluated from

$$E(T) = \int_0^\infty d\epsilon \epsilon N(\epsilon) f_F(\epsilon) \, , \tag{1.9}$$

where

$$f_F(\epsilon) = \frac{1}{e^{(\epsilon-\mu)/k_B T}+1} \tag{1.10}$$

is the Fermi distribution function, while

$$N(\epsilon) \equiv \frac{dG(\epsilon)}{d\epsilon} \tag{1.11}$$

is the density of states (DoS). For a trapped gas one can easily show that at zero temperature

$$E(0) = \frac{3}{4}N\varepsilon_F \, , \tag{1.12}$$

while for a homogeneous gas $E(0) = 3N\varepsilon_F/5$. The behaviour of $E(T)$ with temperature is plotted in Fig. 1.2 and compared with the energy of a classical gas, $E_{\rm cl}(T) = 3Nk_BT/2$ — according to the equipartition principle each particle brings an energy equal to $k_BT/2$. We will see in Sect. 1.1.2 how $E(T)$ can be measured in experiments and how, at low enough temperatures, deviations from the classical behaviour can be measured at the on-set of quantum degeneracy.

[1] Note that for a trapped gas $n \sim N(m\bar{\omega}^2/k_BT)^{3/2}$.

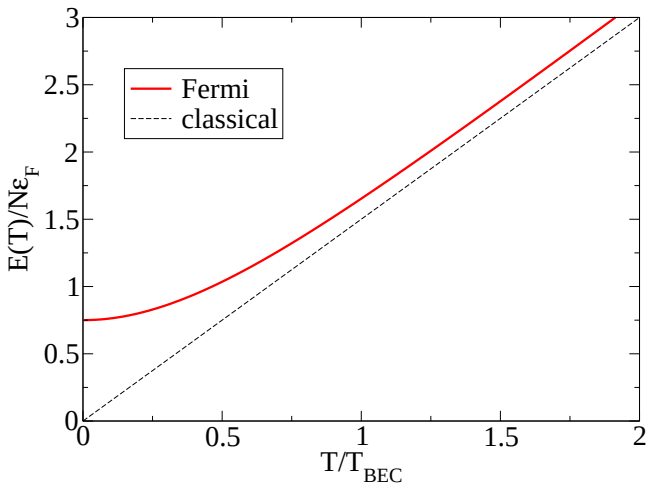

Figure 1.2: Energy per particle of a Fermi gas (red solid line) as a function of temperature, compared with the one of a classical gas (black dashed).

1.1.1 Density profile of a trapped cloud of fermions

In the limit of a large number of atoms N one can make use of a semiclassical description of the gas. In this case the properties of the gas at a given point $\mathbf{r}$ of the trap are assumed to be those of a uniform gas having a density equal to the local density $n(\mathbf{r})$. In this *local density approximation* (LDA) the Fermi distribution function is given by

$$f_F(\mathbf{r},\mathbf{k}) = \frac{1}{\exp[\beta(\epsilon_\mathbf{k} + V(\mathbf{r}) - \mu)] + 1} \ , \tag{1.13}$$

where $\epsilon_\mathbf{k} = \mathbf{k}^2/2m$, $V(\mathbf{r})$ is the harmonic trapping potential, and the chemical potential μ is fixed by the number of particle equation:

$$N = \int d\mathbf{r} n(\mathbf{r}) = \int d\mathbf{r} \int \frac{d\mathbf{k}}{(2\pi)^3} f_F(\mathbf{r},\mathbf{k}) \ . \tag{1.14}$$

In other words, in the LDA, the effect of the trap is absorbed in a redefinition of the chemical potential, which now is a function of space:

$$\mu(\mathbf{r}) = V(\mathbf{r}) - \mu \ . \tag{1.15}$$

Problem: Re-obtain the expression of the Fermi energy for a trapped gas (1.6) making use of (1.14) (**Hint**: the Fermi energy is defined as $\varepsilon_F = \mu(T=0)$).

In the zero temperature limit, the density profile $n(\mathbf{r}) = \int d\mathbf{k}/(2\pi)^3 f_F(\mathbf{r},\mathbf{k})$ is therefore given by

$$n(\mathbf{r}) = \frac{1}{6\pi^2} \left[2m(\varepsilon_F - V(\mathbf{r}))\right]^{3/2} \ , \tag{1.16}$$

if $V(\mathbf{r}) < \varepsilon_F$ and zero otherwise, where $\varepsilon_F = \mu(T=0)$. The LDA is therefore equivalent to consider a local Fermi momentum $k_F(\mathbf{r})$ such that $k_F^2(\mathbf{r})/2m +$

$V(\mathbf{r}) = \mu$. The profile (1.16) can therefore be also obtained from the gas density of a homogeneous system:

$$n = \frac{k_F^3}{6\pi^2} \ . \tag{1.17}$$

1.1.2 Experiments on quantum degenerate Fermi gases

As it will be explained in detail in Sec. 2.1.1, the Pauli exclusion principle forbids s-wave interaction for identical fermions. In other words the total wave-function for two identical fermions,

$$\Psi_{\rm tot}(1,2) = \psi(\mathbf{r}_1, \mathbf{r}_2) \ , \chi_{\rm spin} \tag{1.18}$$

is characterised by a symmetric spin component $\chi_{\rm spin}$ and therefore the wave function describing the relative motion $\psi(\mathbf{r}_1, \mathbf{r}_2)$ has to be antisymmetric under the exchange of the particles (i.e., only angular momenta $\ell = 1, 3, \ldots$ are allowed). As a consequence, at low temperatures, identical fermions do not collide, therefore making difficult to apply the the principle of evaporative cooling (see Appendix C) and reach quantum degeneracy. Alternative experimental approaches to the ones used for bosons have been therefore used to cool fermions down:

1. *Simultaneous cooling:* simultaneous trapping of different spin $|F, m_F\rangle$ (see Appendix A) species: The Pauli principle does not suppress the s-wave scattering between different spin component.

2. *Sympathetic cooling:* simultaneous trapping of a mixture of bosonic and fermionic atoms, such as ^{7}Li-^{6}Li (Rice and ENS) and ^{87}Rb-^{40}K (LENS): Fermions are cooled by means of the boson, i.e. by evaporating bosonic atoms, fermionic atoms cools via thermal contact.

Once the mixture is cooled down to degeneracy temperatures, the second component, whether a second spin state or the bosonic atoms, are eliminated from the trap by applying a radio-frequency (RF) impulse.

The main idea and results of the experiments on quantum degenerate (one-component) Fermi gases will be discussed to some extent during the lectures. For reference to relevant papers see the captions of Figs. 1.3, 1.4, 1.5.

1.2 Pairing instability

In the remaining of this first lecture, we want to discuss how the non-interacting scenario for identical (one-component) Fermi gases can dramatically change in presence of a weak attractive interaction if one considers two-component mixtures. Details about how atom interact, about why in order to have interaction between identical atomic fermions one has to prepare them in a mixture of two different internal (hyperfine) states, and details about how the interaction strength can be changed by an external homogeneous magnetic field (Feshbach resonance), will be discussed in the next lecture. Therefore, for the moment being, let us consider as a reference example the case of electrons in a metal and explain the basics of the transition to a superfluid phase — note that much more detailed explanations about the pairing instability mechanism and the BCS theory will be given during the course of Derek Lee, therefore this section is only a reminder.

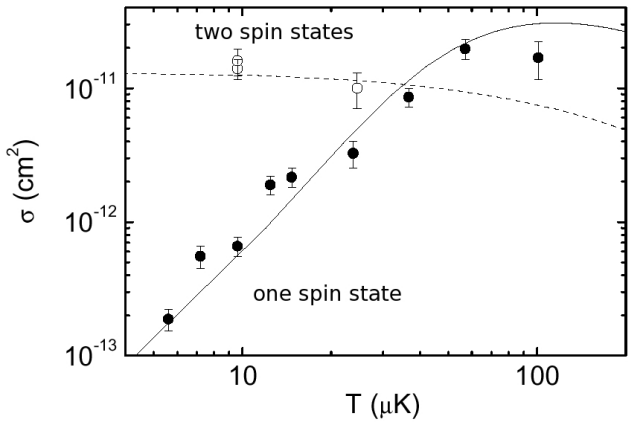

Figure 1.3: Temperature dependence of the cross section of a mixture of atoms in two-spin states and in a single-spin state (from [12]; see also [19]).

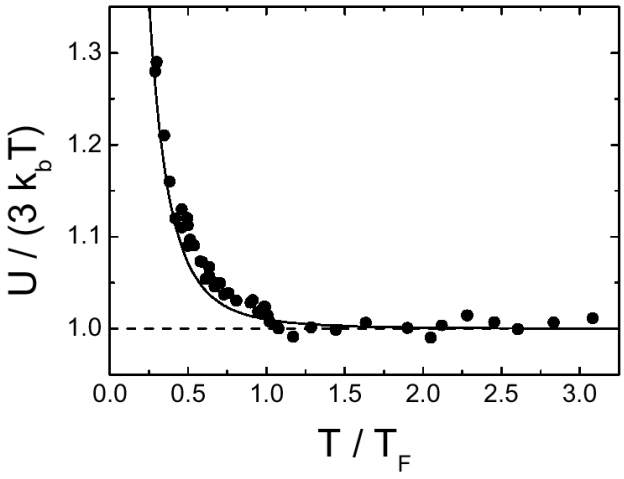

Figure 1.4: Energy of the Fermi gas compared to the energy of a classical gas versus T/T_F (from [12]; see also [19]).

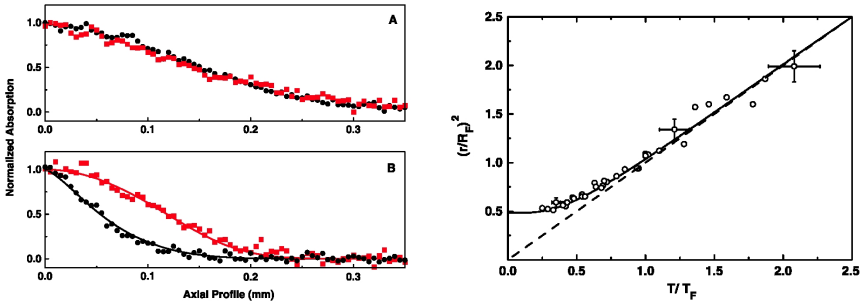

(a) (b)

Figure 1.5: Evidence of Fermi pressure (from [37]).

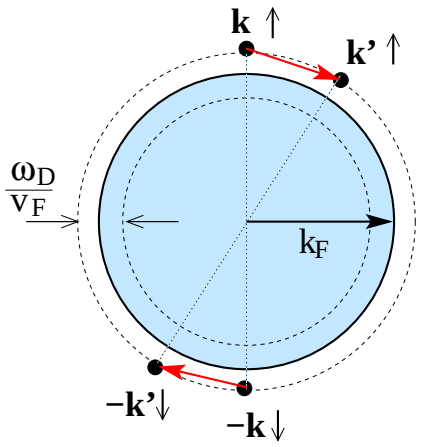

Figure 1.6: Coupling between electron pair states with opposite spin and momenta in the one-pair Cooper problem and typical scattering process $\mathbf{k} \mapsto \mathbf{k}'$ due to the pairing potential $U_{\mathbf{k},\mathbf{k}'}$.

1.2.1 The one-pair Cooper problem

It was first Leon Cooper's idea in 1956 [6] (see also [34]) that an even arbitrarily weak attraction can bind pairs of electrons into a bound state. The toy model used by Cooper is the one of a pair of electrons which interact above a non-interacting Fermi sphere — the background electrons enter the problem only by blocking, via the Pauli exclusion principle, the occupation of the states below the Fermi energy:

$$\left[-\frac{1}{2m}(\nabla_1^2+\nabla_2^2)+U(\mathbf{r}_1-\mathbf{r}_2)\right]\psi(\mathbf{r}_1,\mathbf{r}_2)=(\epsilon+2\varepsilon_F)\psi(\mathbf{r}_1,\mathbf{r}_2)\ . \tag{1.19}$$

It is useful to introduce relative $\mathbf{r}=\mathbf{r}_1-\mathbf{r}_2$ and centre of mass $\mathbf{R}=(\mathbf{r}_1+\mathbf{r}_2)/2$ coordinates

$$\psi(\mathbf{r}_1,\mathbf{r}_2)=\varphi(\mathbf{r})e^{i\mathbf{R}\cdot\mathbf{q}}\chi_{\text{spin}}\ .$$

We will start considering the $\mathbf{q}=0$ case and later on show that finite $\mathbf{q}$ states correspond to higher energy states. As the spin of the electrons is concerned, one can either be in a triplet or singlet state:

$$\chi^S_{\text{spin}}=\frac{|\uparrow\rangle|\downarrow\rangle-|\downarrow\rangle|\uparrow\rangle}{\sqrt{2}} \qquad \chi^T_{\text{spin}}=\begin{cases}\dfrac{|\uparrow\rangle|\downarrow\rangle+|\downarrow\rangle|\uparrow\rangle}{\sqrt{2}}\\ |\uparrow\rangle|\uparrow\rangle\\ |\downarrow\rangle|\downarrow\rangle\end{cases} \tag{1.20}$$

$$\varphi(\mathbf{r})=\varphi(-\mathbf{r}) \qquad \varphi(\mathbf{r})=-\varphi(-\mathbf{r})\ .$$

It is possible to show that the state with lowest energy is the spin singlet one.

Considering the Fourier expansion of the relative motion wave-function,

$$\varphi(\mathbf{r})=\frac{1}{V}\sum_{\mathbf{k}}\varphi_{\mathbf{k}}e^{i\mathbf{k}\cdot\mathbf{r}}=\frac{1}{V}\sum_{\mathbf{k}}\varphi_{\mathbf{k}}e^{i\mathbf{k}\cdot\mathbf{r}_1-i\mathbf{k}\cdot\mathbf{r}_2}\ ,$$

the pair wave-function is made up of plane waves of equal and opposite momenta (see Fig. 1.6) and the Schrödinger equation now reads:

$$2\xi_{\mathbf{k}}\varphi_{\mathbf{k}} + \frac{1}{V}\sum_{\mathbf{k}'} U_{\mathbf{k},\mathbf{k}'}\varphi_{\mathbf{k}'} = \epsilon\varphi_{\mathbf{k}} \ , \tag{1.21}$$

where $\xi_{\mathbf{k}} = \epsilon_{\mathbf{k}} - \varepsilon_F$ and $U_{\mathbf{k},\mathbf{k}'} = \int d\mathbf{r} U(\mathbf{r}) e^{i\mathbf{r}\cdot(\mathbf{k}-\mathbf{k}')}$. Equation (1.21) can be easily obtained multiplying r.h.s. and l.h.s. of (1.19) by $\int d\mathbf{r} e^{-i\mathbf{k}'\cdot\mathbf{r}}$ and by making use of the orthonormality condition $\int d\mathbf{r} e^{i(\mathbf{k}-\mathbf{k}')\cdot\mathbf{r}} = V\delta_{\mathbf{k},\mathbf{k}'}$.

In general it is not possible to find an analytical solution of Eq. (1.21) (see [34] for the case of a *separable potential*, $U_{\mathbf{k},\mathbf{k}'} \equiv g w^*_{\mathbf{k}'} w_{\mathbf{k}}$). We will consider the simplest case where a maximum frequency ω_D (Deby frequency) can be exchanged between electrons via a phonon:

$$U_{\mathbf{k},\mathbf{k}'} = \begin{cases} g & |\xi_{\mathbf{k}}|, |\xi_{\mathbf{k}'}| < \omega_D \\ 0 & \text{otherwise} \ , \end{cases} \tag{1.22}$$

and where the interaction between the electrons is attractive, $g \equiv -\lambda < 0$. In conventional superconductors, the attractive interaction between electrons is due do the exchange of lattice vibrations (i.e., phonons): A first electron polarises the medium by dislocating (attracting) lattice ions, causing a second electron to be attracted by the region of the distorted potential. The retarded nature of the phonon interaction allows the electrons to avoid repelling each other because of the Coulomb interaction.

In the case of the interaction (1.22) we can rewrite (1.21) as

$$\varphi_{\mathbf{k}} = \frac{\lambda}{2\xi_{\mathbf{k}} - \epsilon}\frac{1}{V}\sum_{\mathbf{k}'}^{|\xi_{\mathbf{k}'}|<\omega_D} \varphi_{\mathbf{k}'} \ ,$$

where the sum is restricted to an energy interval ω_D around the Fermi surface ε_F; summing over $\mathbf{k}$ on both sides, one obtains the following equation for the eigenenergy ϵ:

$$1 = \lambda\frac{1}{V}\sum_{\mathbf{k}}^{|\xi_{\mathbf{k}}|<\omega_D} \frac{1}{2\xi_{\mathbf{k}} - \epsilon} = \lambda\int_{\varepsilon_F}^{\varepsilon_F+\omega_D} de\mathcal{N}(e)\frac{1}{2(e-\varepsilon_F) - \epsilon} \ ,$$

where the DoS per unit volume $\mathcal{N}(e) = N(e)/V$ has been introduced in (1.11):

$$\frac{1}{V}\sum_{\mathbf{k}} = \int \frac{d\mathbf{k}}{(2\pi)^3} = \int_0^\infty de\mathcal{N}(e) \qquad \mathcal{N}(e) = \frac{m^{3/2}\sqrt{e}}{\sqrt{2}\pi^2} \ . \tag{1.23}$$

The eigenvalue equation can be easily solved assuming that the DoS is approximatively constant at the Fermi surface, $\mathcal{N}(e) \simeq \mathcal{N}(\varepsilon_F)$, giving the solution $\epsilon = -2\omega_D e^{-2/\lambda\mathcal{N}(\varepsilon_F)}/(1 - e^{-2/\lambda\mathcal{N}(\varepsilon_F)})$. In the weak coupling approximation, $\lambda\mathcal{N}(\varepsilon_F) \ll 1$, this reduces to:

$$\epsilon \simeq -2\omega_D e^{-\frac{2}{\lambda\mathcal{N}(\varepsilon_F)}} \ . \tag{1.24}$$

Therefore we can conclude that a bound state always exists, even for any arbitrarily weak coupling strength λ as long as the potential $U_{\mathbf{k},\mathbf{k}'}$ is attractive near the Fermi surface.

In addition one can evaluate the mean square radius of the pair wave function (the size of the *Cooper pair*):

$$\overline{r^2} = \frac{\int d\mathbf{r} r^2 |\varphi(\mathbf{r})|^2}{\int d\mathbf{r} |\varphi(\mathbf{r})|^2} \simeq \frac{4}{3} \frac{v_F^2}{\epsilon^2} \ .$$

We will see later that the binding energy ϵ is of the same order of magnitude than the critical temperature to a superconducting phase $T_{\rm BCS}$ resulting from the macroscopically occupation of Cooper pairs. Therefore, for typical values of the binding energy $\epsilon \simeq k_B T_{\rm BCS} \sim 10$K and the Fermi velocity $v_F \sim 10^8$cm/s, one has a mean radius of about $(\overline{r^2})^{1/2} \sim 10^4 \mathring{A}$, which is of the same order of the Pippard coherence length.

This result has been extremely important in explaining the mechanism at the origin of superconductivity: Cooper [6] suggested that the *instability* of the normal phase to *pairing* of electrons with opposite momenta and spin is associated with the occurrence of a superconducting state. However, in reality superconductors differ in a fundamental way from the one-pair model. Cooper bound pairs are not well separated in space but instead, as explained in Sec. 1.3, are strongly overlapping: There are typically around 10^{11} other electrons within a 'coherence volume' $(\overline{r^2})^{3/2}$ and therefore there are many Cooper bound pairs which centre of mass is in between a given pair. Superconductivity is not a two-body properties, rather a collective phenomena. We will see in Sec. 1.3 how this has been explained in the correct many-body theory framework by a seminal work due to Bardeen, Cooper and Schrieffer (BCS).

Finally one can easily show that, with a small centre of mass momentum $\mathbf{q}$, the binding energy is given by

$$|\epsilon(\mathbf{q})| \simeq |\epsilon| - \frac{v_F |\mathbf{q}|}{2} \ , \tag{1.25}$$

and therefore the pair binding energy is reduced by a drift of the pair.

We will see later that in an ordinary superconductor the critical temperature described by the BCS theory is proportional to the pair binding energy in (1.24), i.e. $\epsilon \simeq k_B T_{\rm BCS}$. In other words, in a BCS superconductor the energy and temperature scales at which (Cooper) pairs form and condense is the same (*pairing instability*). We will also see that this behaviour is very different from the condensation of composite bosons formed of tightly bound fermionic molecules, where the energy and temperature for dissociating a bound pair are much higher that the BEC temperature of condensation.

1.3 BCS theory

The nature of the ordering between electrons in a metal at the basis of superconductivity was explained by Bardeen, Cooper and Schrieffer in 1957 [3]. As explained in the previous section, already the instability of electron pairs to form bound pairs of states with opposite spin and momentum, $\mathbf{k} \uparrow$ and $-\mathbf{k} \downarrow$, in the vicinity of the Fermi surface was proposed by Cooper [6]. The BCS theory elucidate how the same pairing mechanism can explain the superconducting behaviour on a many-body collective level. The BCS theory (see, e.g., Refs. [1, 34, 36] for detailed reference books) will be explained during the

course of Derek Lee, therefore here I will give only the basic elements. Later, in Sec. 2.3 we will analyse in more detail some aspects in relation to the BEC-BCS crossover theory.

The starting point is the Hamiltonian with a contact attractive ($g \equiv -\lambda < 0$) potential,

$$\hat{H} = \sum_{\mathbf{k},\sigma=\uparrow,\downarrow} \epsilon_{\mathbf{k}} c^\dagger_{\mathbf{k}\sigma} c_{\mathbf{k}\sigma} + \frac{g}{V} \sum_{\mathbf{k},\mathbf{k}',\mathbf{q}} c^\dagger_{\mathbf{k}+\mathbf{q}/2\uparrow} c^\dagger_{-\mathbf{k}+\mathbf{q}/2\downarrow} c_{-\mathbf{k}'+\mathbf{q}/2\downarrow} c_{\mathbf{k}'+\mathbf{q}/2\uparrow} \ , \quad (1.26)$$

where the interaction is effective on an interval of width ω_D around the Fermi surface (see Eq. (1.22) and Fig. 1.6). The number of particles is fixed by introducing the Fermi energy ε_F and considering $\hat{H} - \varepsilon_F \hat{N}$, where

$$\hat{N} = \sum_{\mathbf{k},\sigma=\uparrow,\downarrow} c^\dagger_{\mathbf{k}\sigma} c_{\mathbf{k}\sigma} \ .$$

On the basis of the Copper pairing instability argument, the BCS theory starts from the assumption (*pairing Ansatz*) that the ground state of the Hamiltonian (1.26) $|\psi\rangle$ is described by the presence of Cooper pairs with opposite spin and momentum. In this case, the order parameter, i.e. the expectation value

$$\Delta \equiv= -\frac{g}{V} \sum_{\mathbf{k}} \langle \psi | c_{-\mathbf{k}\downarrow} c_{\mathbf{k}\uparrow} | \psi \rangle \ , \quad (1.27)$$

is non zero. With this assumption, one can neglect all the other correlations than the pair correlations introduced by the order parameter Δ and consider the *mean-field* (Bogoliubov) Hamiltonian

$$\hat{H} - \varepsilon_F \hat{N} \simeq \sum_{\mathbf{k}} \begin{pmatrix} c^\dagger_{\mathbf{k}\uparrow} & c_{-\mathbf{k}\downarrow} \end{pmatrix} \begin{pmatrix} \xi_{\mathbf{k}} & -\Delta \\ -\Delta & -\xi_{\mathbf{k}} \end{pmatrix} \begin{pmatrix} c_{\mathbf{k}\uparrow} \\ c^\dagger_{-\mathbf{k}\downarrow} \end{pmatrix} + \sum_{\mathbf{k}} \xi_{\mathbf{k}} - \frac{\Delta^2}{g} V \ . \quad (1.28)$$

Problem: Show that the mean-field Hamiltonian (1.28) can be diagonalised by making use of the unitary transformation:

$$\begin{pmatrix} \gamma_{\mathbf{k}\uparrow} \\ \gamma^\dagger_{-\mathbf{k}\downarrow} \end{pmatrix} = \begin{pmatrix} \cos\theta_{\mathbf{k}} & \sin\theta_{\mathbf{k}} \\ \sin\theta_{\mathbf{k}} & -\cos\theta_{\mathbf{k}} \end{pmatrix} \begin{pmatrix} c_{\mathbf{k}\uparrow} \\ c^\dagger_{-\mathbf{k}\downarrow} \end{pmatrix} \ . \quad (1.29)$$

Show that the unitary transformation conserves the anti-commutation relations for the (Bogoliubov) quasi-particle operators $\gamma_{\mathbf{k}\sigma}$ and that the quasi-particle energy is given by $E_{\mathbf{k}} = \sqrt{\xi^2_{\mathbf{k}} + \Delta^2}$, i.e.:

$$\hat{H} - \varepsilon_F \hat{N} \simeq \sum_{\mathbf{k},\sigma=\uparrow,\downarrow} E_{\mathbf{k}} \gamma^\dagger_{\mathbf{k}\sigma} \gamma_{\mathbf{k}\sigma} + \sum_{\mathbf{k}} (\xi_{\mathbf{k}} - E_{\mathbf{k}}) - \frac{\Delta^2}{g} V \ . \quad (1.30)$$

It is clear from the Bogoliubov transformation (1.29) that the ground state of the Hamiltonian is uniquely given by the state that is annihilated by the quasi-particle operators $\gamma_{\mathbf{k}\sigma}$:

$$|\psi\rangle = \prod_{\mathbf{k}} \gamma_{-\mathbf{k}\downarrow} \gamma_{\mathbf{k}\uparrow} |0\rangle \propto \prod_{\mathbf{k}} \left(\cos\theta + \sin\theta c^\dagger_{\mathbf{k}\uparrow} c^\dagger_{-\mathbf{k}\downarrow} \right) |0\rangle \ .$$

Therefore, instead than introducing the mean-field Hamiltonian (1.28) we could have alternatively used a variational approach, minimising the expectation value of the full Hamiltonian $\langle\psi|\hat{H}-\varepsilon_F\hat{N}|\psi\rangle$ over the variational parameter $\theta_{\mathbf{k}}$. We will follow this route later in Sec. 2.3.1 to find the gap (or self-consistent) equation for the order parameter; in both cases one obtains:

$$\Delta_{\rm BCS} = -\frac{g}{V}\sum_{\mathbf{k}}\langle\psi|c_{-\mathbf{k}\downarrow}c_{\mathbf{k}\uparrow}|\psi\rangle = -\frac{g}{2V}\sum_{\mathbf{k}}\sin 2\theta_{\mathbf{k}} = -\frac{g}{V}\sum_{\mathbf{k}}\frac{\Delta_{\rm BCS}}{2E_{\mathbf{k}}}\ .$$

Problem: Assuming that the pairing interaction $g=-\lambda$ extends only over an interval ω_D around the Fermi surface, show that the gap equation can be solved to give:

$$\Delta_{\rm BCS} = \frac{\omega_D}{\sinh(1/\lambda\mathcal{N}(\varepsilon_F))} \underset{\lambda\mathcal{N}(\varepsilon_F)\ll 1}{\simeq} 2\omega_D e^{-\frac{1}{\lambda\mathcal{N}(\varepsilon_F)}}\ . \tag{1.31}$$

(**Hint:** Remember the relation (1.23) and approximate $\mathcal{N}(e)\simeq\mathcal{N}(\varepsilon_F)$.)

Note that this expression differs for a factor of 2 in the exponential from the one of the binding energy in the Cooper argument in Eq. (1.24).

In order to add the effects of temperature we can come back to the expression (1.30) of the mean-field energy in terms of the Bogoliubov quasi-particle operators and observe that, at zero temperature, the thermodynamical free energy potential $f(\Delta)\equiv\langle\psi|\hat{H}-\varepsilon_F\hat{N}|\psi\rangle$ corresponds to fill all the states $\mathbf{k}$ with $E_{\mathbf{k}}>0$ (i.e. all!) with Cooper pairs: [2]

$$f(\Delta)\equiv\langle\psi|\hat{H}-\varepsilon_F\hat{N}|\psi\rangle = \underbrace{\sum_{\mathbf{k}}\Theta(-E_{\mathbf{k}})E_{\mathbf{k}}}_{=0} + \sum_{\mathbf{k}}(\xi_{\mathbf{k}}-E_{\mathbf{k}}) - \frac{\Delta^2}{g}V\ . \tag{1.32}$$

At finite temperature one has instead to broaden the Θ-function distribution and one can show that the free energy potential has the form

$$f(\Delta,T) = -\sum_{\mathbf{k}}\frac{1}{\beta}\ln\left(1+e^{-\beta E_{\mathbf{k}}}\right) + \sum_{\mathbf{k}}(\xi_{\mathbf{k}}-E_{\mathbf{k}}) - \frac{\Delta^2}{g}V\ , \tag{1.33}$$

where $\beta=1/k_BT$. One can easily show that, in the limit $\beta\to\infty$ one recovers the zero temperature expression for the free energy potential. Now the gap equation, $\partial f(\Delta,T)/\partial\Delta=0$, will be temperature dependent,

$$-\frac{1}{g\mathcal{N}(\varepsilon_F)} = \int_0^{\omega_D} d\xi\frac{\tanh\left[\beta E(\xi)/2\right]}{E(\xi)}\ , \tag{1.34}$$

where $E(\xi)=\sqrt{\xi^2+\Delta^2}$, and, by considering the $\Delta\to 0$ limit, one can evaluate the transition temperature to the BCS state (exercise):

$$k_BT_{\rm BCS}\simeq\omega_D e^{-\frac{1}{\lambda\mathcal{N}(\varepsilon_F)}}\ . \tag{1.35}$$

[2] Note that clearly the gap equation coincide with the minimisation of $f(\Delta)$, i.e. $\partial f/\partial\Delta=0$.

Chapter 2

Lecture II: Feshbach resonances & BEC-BCS crossover

We have seen in Sec. 1.1.2 that, when a gas of Fermi atoms is prepared in the same internal spin state, then, at low temperatures, the gas is completely non interacting. As we will explain below, the case of a mixture of fermions prepared in two different hyperfine states is different. We will show that in the case of two-component Fermi gases, a measure of their interaction strength is given by the dimensionless product

$$\frac{1}{k_F a} ,$$

where a is the s-wave *scattering length* (see Sec. 2.1) andk_F is the Fermi momentum of the gas. It is easy to show that for a uniform gas containing a mixture of equal densities of the same specie fermions in two different states, the product $k_F a$ is the only quantity of interest. In fact, at zero temperature the kinetic energy per particle is given by the Fermi energy, $\varepsilon_F = k_F^2/2m$, while the interaction energy per particle is given by nU_0, where n is the particle density for one component. We will show that the effective interaction strength between the atoms is related to the scattering length by $U_0 = 4\pi a/m$. Therefore the ratio between the interaction energy to the Fermi energy, by using (1.17), is proportional to $k_F a$ (i.e. $nU_0/\varepsilon_F = 4k_F a/3\pi$).

After introducing basic concepts on atomic interactions, we will see in Sec. 2.2 how the interaction strength between atoms can be tuned by changing an external homogeneous magnetic field, via a mechanism known as *Feshbach resonance*. The tunability of the scattering length from a regime of attractive interaction ($a < 0$) between the fermions to a regime where fermions form bound bosonic molecules (and the effective interaction between the fermions is repulsive, $a > 0$) will allow to study in Sec. 2.3 the *crossover* between a BCS state of strongly overlapping Cooper pairs (as we studied in Sec. 1.3) to a state where instead tightly bound molecules formed by fermionic pairs can undergo usual BEC. The pioneering experiments in which this crossover has been realised will be finally discussed in Sec. 2.4.

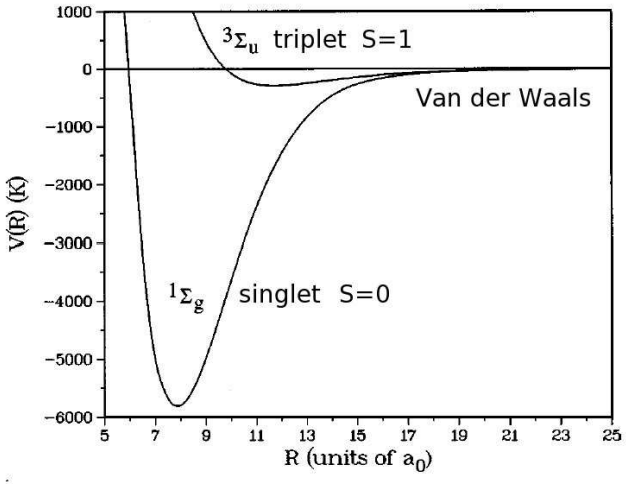

Figure 2.1: Characteristic singlet and triplet scattering potential for ^{87}Rb.

2.1 Interactions between atoms

As explained in more detail in the App. C, quantum degeneracy in alkali gases can be reached only in a regime of *metastability* rather than true thermal equilibrium. This is because the real equilibrium phase of interacting alkali atoms at the temperatures and densities at which quantum degeneracy can be reached would be a crystalline solid phase rather than the one of the gas. Therefore alkali gases have to be kept in conditions of extreme diluteness, where, on the time scales relevant for the experiments, 3-body collisions can be neglected and where the collisional properties of the atoms are determined, as we will see, by the s-wave scattering length only. In this regime, the particle separation is much larger that the s-wave scattering length and typical values are given by:

$$\bar{r} \sim n^{-1/3} \sim 100\text{nm} \qquad\qquad a \sim 100 a_0 \sim 5\text{nm} \ ,$$

where $a_0 = 0.529\mathring{A}$ is the Bohr radius. Two-body collisions are essential to ensure thermalization of the cloud, allow to apply cooling techniques such as evaporative cooling (see App. C), and it is thanks to interaction effects that two-component Fermi mixtures to undergo a phase transition to a superfluid phase. [1]

When two alkali atoms are very far apart, each of them is characterised by a given *hyperfine state* $|F, m_F\rangle$ (see appendix A). At *large distances*, two atoms interact via a weak Van der Waals attraction (due to the electronic dipole-dipole interaction between the atoms),

$$U_{\text{VdW}}(r) = -\frac{C_6}{r^6} \ ,$$

which cannot change the hyperfine state the atoms are initially at. In contrast, at *small distances* the interaction is predominantly determined by the valence

[1] Note however that for a BEC of dilute bosonic alkali atoms, interaction effects do not strongly modify the results obtained for an ideal gas as, e.g., the critical temperature and the condensate fraction are concerned.

electron and one can show that the interaction potential is different depending whether the two valence electrons form a singlet or a triplet state (1.20) (see Fig. 2.1). Therefore, since the operators $1/4 - \hat{\mathbf{S}}_1 \cdot \hat{\mathbf{S}}_2$ and $3/4 + \hat{\mathbf{S}}_1 \cdot \hat{\mathbf{S}}_2$ are respectively projectors on the singlet ($S = 0$) and triplet ($S = 1$) spin component (N.B. $\hat{\mathbf{S}}_1 \cdot \hat{\mathbf{S}}_2 = \hat{\mathbf{S}}^2/2 - 3/4$ and $\hat{\mathbf{S}}^2|S, S_z\rangle = S(S+1)|S, S_z\rangle$), one can write the interaction potential at short distances in the form:

$$\hat{H}_{\rm int} = \frac{U_s(\mathbf{r}) + 3U_t(\mathbf{r})}{4} + \left[U_t(\mathbf{r}) - U_s(\mathbf{r})\right] \hat{\mathbf{S}}_1 \cdot \hat{\mathbf{S}}_2 \ . \tag{2.1}$$

As a consequence, the hyperfine levels can now be mixed (*multiple channel* problem), unless the atoms initially occupy the *doubly polarised states* $|F = I + 1/2, m_F = \pm(I + 1/2)\rangle$ (see page 42). In fact, in this case,

$$|F = I + 1/2, m_F = \pm(I + 1/2)\rangle = |m_I = \pm I, m_S = \pm 1/2\rangle \ ,$$

therefore both valence electrons have spin either $\uparrow$ or $\downarrow$ and therefore only the triplet part of the potential contributes (*single channel* problem).

In the general case, the term

$$\hat{\mathbf{S}}_1 \cdot \hat{\mathbf{S}}_2 = \hat{\mathbf{S}}_{1z}\hat{\mathbf{S}}_{2z} + \frac{1}{2}\hat{\mathbf{S}}_{1+}\hat{\mathbf{S}}_{2-} + \frac{1}{2}\hat{\mathbf{S}}_{1-}\hat{\mathbf{S}}_{2+}$$

in (2.1) can scatter the atoms from two initial hyperfine levels into two other final hyperfine levels; the selection rules for the scattering is governed by the matrix element ${}_{1,i}\langle F, m_F| \otimes_{2,i} \langle F, m_F|\hat{H}_{\rm int}|F, m_F\rangle_{1,f} \otimes |F, m_F\rangle_{2,f}$.

Problem: Considering the case of ^{40}K (see problem at page 44), evaluate the final state in which two atoms initially in $|9/2, -9/2\rangle_1 \otimes |9/2, -7/2\rangle_2$ can scatter into.

Answer: Remembering that a hyperfine level for a single atom $|F, m_F\rangle$ is a superposition of the following eigenstates of $\hat{I}_z$ and $\hat{S}_z$ (as explained in detail in App. A, in presence of a magnetic field, $m_F = m_I \pm 1/2$ is the only good quantum number, while F is only a label),

$$|F, m_F = m_I \pm 1/2\rangle = \cos\theta|m_I, \pm 1/2\rangle + \sin\theta|m_I \pm 1, \mp 1/2\rangle \ ,$$

and noticing that $\hat{\mathbf{S}}_1 \cdot \hat{\mathbf{S}}_2$ conserves only $m_{F\rm tot} = m_{F1} + m_{F2}$ (i.e., $[\hat{F}_{z1} + \hat{F}_{z2}, \hat{\mathbf{S}}_1 \cdot \hat{\mathbf{S}}_2] = 0$), the only scattering to a different state which is allowed is

$$|9/2, -9/2\rangle_1 \otimes |9/2, -7/2\rangle_2 \mapsto |9/2, -9/2\rangle_1 \otimes |7/2, -7/2\rangle_2 \ .$$

2.1.1 s-wave scattering length

Let's consider for the moment the case of (spinless) distinguishable particles, including later the effects of statistics. In order to consider the scattering of two particles, we concentrate on the relative motion ($\mathbf{r} = \mathbf{r}_1 - \mathbf{r}_2$) and we look for the eigenstates of the scattering problem,

$$\left[-\frac{\nabla^2}{2m_r} + U(\mathbf{r})\right] \psi_{\mathbf{k}}(\mathbf{r}) = \epsilon_{r\mathbf{k}} \psi_{\mathbf{k}}(\mathbf{r}) \ , \tag{2.2}$$

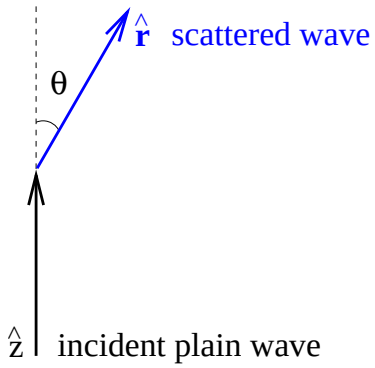

Figure 2.2: Scattering of an incoming plane wave e^{ikz} into a scattered wave $f(\theta)e^{ikr}/r$ in the direction $\hat{\mathbf{r}}$.

with a defined positive energy, $\epsilon_{r\mathbf{k}} = \mathbf{k}^2/2m_r$ (m_r being the reduced mass, $m_r = m_1 m_2/(m_1 + m_2)$). In general we are not interested for the moment in the specific shape of the scattering potential, $U(\mathbf{r})$, but will only assume that is characterised by some range R_e and that $U(\mathbf{r}) \to 0$ when $|\mathbf{r}| \to \infty$ fast enough. At large distances, $|\mathbf{r}| \gg R_e$, we look for a solution of the form (see Fig. 2.2):

$$\psi_{\mathbf{k}}(\mathbf{r}) = e^{ikz} + f(\theta)\frac{e^{ikr}}{r} \,. \tag{2.3}$$

In general, one should expect the scattering amplitude $f(\theta)$ to be also a function of $\hat{z}$ and $\hat{\mathbf{r}}$. However, we have assumed that the scattering process is spherically symmetric, $U(\mathbf{r}) = U(r)$. $f(\theta)$ defines the scattering cross section

$$d\sigma \equiv |f(\theta)|^2 d\Omega = |f(\theta)|^2 \sin\theta d\theta d\varphi \,, \tag{2.4}$$

and moreover the s-wave scattering length is defined as

$$a \equiv -\lim_{k\to 0} f(\theta) \qquad \Leftrightarrow \qquad \lim_{k\to 0} \psi_{\mathbf{k}}(\mathbf{r}) \propto 1 - \frac{a}{r} \,. \tag{2.5}$$

The sign of the scattering length determines if the effective interaction between the atoms is either attractive ($a < 0$) or repulsive ($a > 0$). In fact, as shown in Sec. B.1, in the Born approximation

$$a_{\text{Born}} = \frac{2m_r}{4\pi}\int d\mathbf{r} U(\mathbf{r}) \,. \tag{2.6}$$

For indistinguishable atoms (in the same hyperfine spin state) one has that for bosons the wave-function $\psi_{\mathbf{k}}(\mathbf{r})$ has to be symmetric under the particle exchange, $\mathbf{r} \mapsto -\mathbf{r}$, while for fermions has to be antisymmetric. As a consequence, as $\mathbf{r} \mapsto -\mathbf{r}$ requires that simultaneously ($r \mapsto r, \theta \mapsto \pi - \theta, \varphi \mapsto \varphi + \pi$) one has to either symmetrise of anti-symmetrise the wave-function according to:

$$\psi^{B,F}_{\mathbf{k}}(\mathbf{r}) = e^{ikz} \pm e^{-ikz} + [f(\theta) \pm f(\pi - \theta)]\frac{e^{ikr}}{r} \,.$$

Therefore, while for bosons the scattering cross section is given by $\sigma = 8\pi a^2$, for fermions (prepared in the same hyperfine state) $\sigma = 0$: *A one-component Fermi gas does not allow s-wave scattering at low energies.*

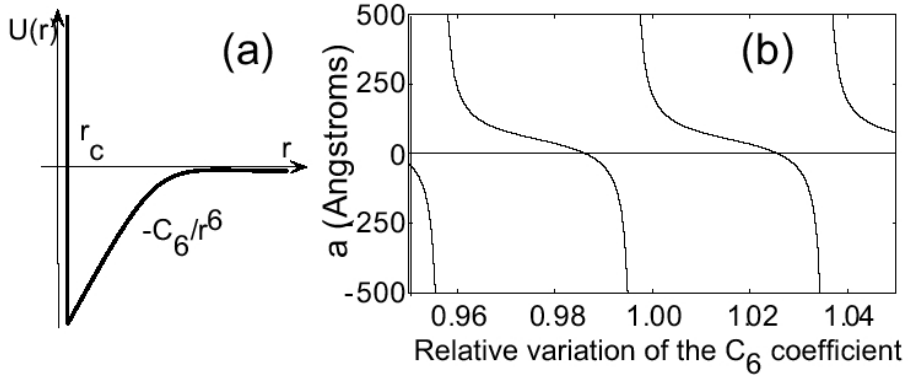

Figure 2.3: Truncated Van der Waals potential and associated scattering length (from [7]). The (quasi-period) variation of the scattering length depends critically on the C_6 coefficient of the Van der Waals tail potential $U_{VdW}(r)$ and a small change in C_6 can introduce a new bound state in the potential, when the scattering length changes from $-\infty$ to ∞. These types of variations in short-range scattering potential are quite general.

Basic elements on how to evaluate the scattering length a given a scattering potential $U(\mathbf{r})$ are explained in App. B together with the example of the square potential well (see Fig. B.2 in App. B). In general one has these following main features for the low energies scattering properties off a potential of the type shown in Fig. 2.1:

1. The sign of the scattering length and therefore of the low energy effective interaction depends on the energy of the highest bound state;

2. If the scattering potential is not deep enough to hold a bound state, the s-wave scattering length is negative, $a < 0$, corresponding to an effective *attractive* interaction between the atoms;

3. If the parameters of the potential (e.g. the depth) can be changed in such a way that eventually it can hold a bound state, then the scattering length becomes positive, $a > 0$ (corresponding to an effective *repulsive* interaction between the atoms), going from $-\infty$ to $+\infty$ when the bound state first appears;

4. If the potential holds a bound state just below the threshold for dissociation, then one can show that its binding energy has a *universal* form in terms of the scattering length:

$$\epsilon_b = -\frac{1}{2m_r a^2} \ . \tag{2.7}$$

This last property follows from the low-energy form of the wave function for a bound state (see Eq. (B.2))

$$\psi(\mathbf{r}) = A\frac{e^{-r\sqrt{2m_r|\epsilon_b|}}}{r} \ ,$$

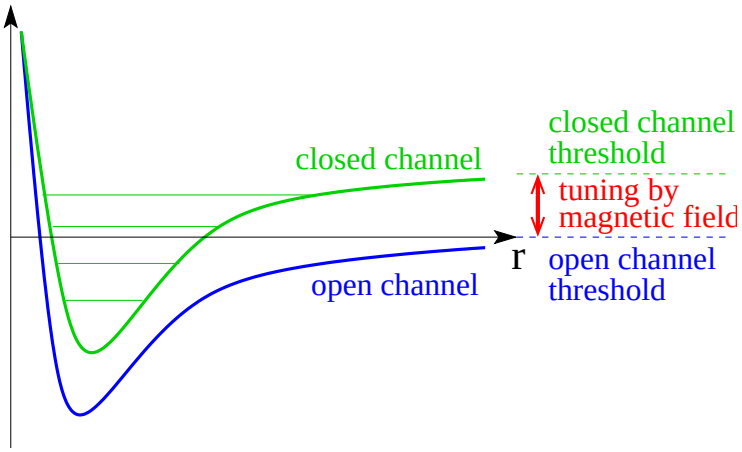

Figure 2.4: Schematic representation of a two-channel model for a Feshbach resonance. The open channel threshold is given by the energy $\epsilon_{\alpha i} + \epsilon_{\beta_i}$, while the closed channel threshold by $\epsilon_{\alpha f} + \epsilon_{\beta f}$. Thanks to the properties of the hyperfine levels in a Zeeman field explained in Sec. A, their relative distance can be tuned by an external uniform magnetic field.

which, when $\epsilon_b \to 0$, becomes

$$\psi(\mathbf{r}) \simeq A\left(\frac{1}{r} - \sqrt{2m_r|\epsilon_b|}\right) ,$$

and compared with (2.5) gives (2.7). For a detailed study of the, e.g., truncated Van der Waals potential (see Fig. 2.3) see Ref. [26].

The considerations above can be extended to the case of scattering between different internal (hyperfine) states. As explained previously at the beginning of Sec. 2.1, two atoms in an initial internal state $|\alpha_i, \beta_i\rangle \equiv |F, m_F\rangle_{1,i} \otimes |F, m_F\rangle_{2,i}$ can be scattered to a different state $|\alpha_f, \beta_f\rangle$ because of the interaction potential (2.1). Aside the selection rules for the final internal state, scattering between an entrance channel $|\mathbf{k}_i; \alpha_i, \beta_i\rangle$ and an exit channel $|\mathbf{k}_f; \alpha_f, \beta_f\rangle$ has to conserve the energy, i.e. $k_i^2/2m_r + \epsilon_{\alpha i} + \epsilon_{\beta_i} = k_f^2/2m_r + \epsilon_{\alpha f} + \epsilon_{\beta f}$. A channel is called *open* if $k^2/2m_r > \epsilon_\alpha + \epsilon_\beta$, conversely is called *closed*. The definition of the scattering amplitude (2.3) can now be generalised to:

$$\psi(\mathbf{r}) = e^{ik_i z}|\alpha_i, \beta_i\rangle + \sum_{\alpha_f, \beta_f} f_{\alpha_i, \beta_i}^{\alpha_f, \beta_f}(\mathbf{k}_i, \mathbf{k}_f)\frac{e^{ik_f r}}{r}|\alpha_f, \beta_f\rangle .$$

2.2 Feshbach resonances

In the previous section we have seen that one way to dramatically change the scattering properties of two interacting particles is by changing the parameters of the scattering potential in order to accommodate or less a bound state close to dissociation threshold. In particular, e.g. by increasing the depth of the potential (see, e.g., the example of square well potential in App. B), we have

seen that the scattering length goes from $-\infty$ to $+\infty$ every time a new bound state is accommodated in the potential well.

Unfortunately changing by external means the parameters of a scattering potential is not possible. However, the elastic scattering properties of a given *open channel* can be dramatically altered if the open channel is coupled to a low-energy bound sate in a second *closed channel* not far from the open one. While here we are going to give only a phenomenological description of the Feshbach resonance mechanism, for a detailed description see, e.g., Ref. [15].

Coupling between the channels follows from the interaction potential (2.1). If two atoms are initially in the scattering state $|\alpha_i, \beta_i\rangle$ they will have some coupling to other scattering states $|\alpha_f, \beta_f\rangle$. When the energy of $|\alpha_f, \beta_f\rangle$ is far apart, the atoms will always emerge in the open channel state $|\alpha_i, \beta_i\rangle$ and their scattering length will be not modified by the coupling to another channel $|\alpha_f, \beta_f\rangle$. In this case the scattering length is given by the *background scattering length*, $a_{\rm bg}$. However, because of the difference in the magnetic moments of the closed and open channels (see Appendix A), by applying an external uniform magnetic field, the position of a closed channel bound state can be varied with respect to the threshold of an open channel (see Fig. 2.4). In this case, the coupling between $|\alpha_i, \beta_i\rangle$ and a bound state of $|\alpha_f, \beta_f\rangle$ can strongly modify the background value of the scattering length. Feshbach resonances are therefore described by a magnetic-field dependent scattering length, according to the relation:

$$a(B) = a_{\rm bg}\left(1 - \frac{\Delta B}{B - B_0}\right) , \tag{2.8}$$

where $a_{\rm bg}$ is the scattering length in absence of coupling between the channels, ΔB is called the width of the resonance and B_0 is the position of the resonance (see Fig. 2.5).

As an aside remark, note that Feshbach resonances works better for two-component Fermi mixture rather then for Bose gases. [2] This is because near the resonance, large values of the scattering length increase the three-body recombination processes (see App. C). For Fermions, the Pauli exclusion principle allows to have longer life-times.

2.3 BEC-BCS crossover

We now come back to the properties of dilute Fermi gases. We have seen in the previous chapter that if a Fermi gas is prepared in the same internal hyperfine state it does not interact at low temperatures and that properties related to quantum degeneracy starts appearing for temperatures below the Fermi temperature T_F defined in Eqs. (1.5) and (1.6). However, if the mixture is prepared in two different hyperfine states (two-component Fermi mixture), atoms in different states can interact and a measure of their coupling strength is given by $k_F a$. Strikingly, we have also seen that the scattering length a can be tuned externally by a homogeneous magnetic field via the Feshbach resonance mechanism. The ability to externally manipulate the interaction strength between the atoms has opened the exciting possibility to study the crossover between two (and at a first sight opposite) regimes: When $a > 0$ and $1/k_F a \gg 1$, the two-species of

[2] Recently mixtures of bosons and fermions, such as ^{87}Rb and ^{40}K, with an interspecies resonance have also been realised [20, 22, 38].

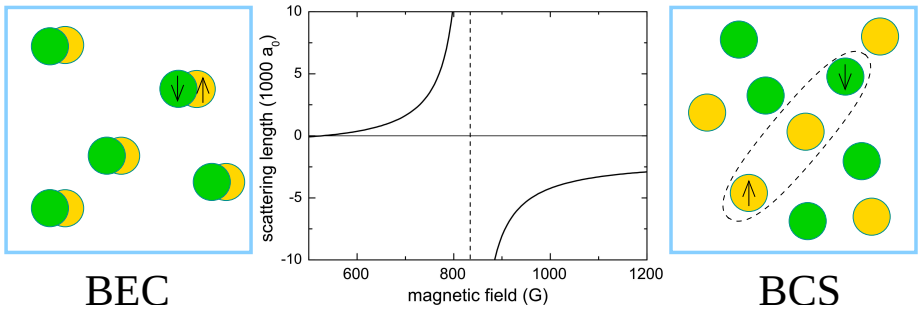

Figure 2.5: BEC-BCS crossover from tightly bound molecules ($1/k_F a \to +\infty$) to loosely bound Cooper pairs ($1/k_F a \to -\infty$) across a Feshbach resonance between the two lowest hyperfine states of ^{6}Li (from [4]): In this case, the resonance is at $B = 834$G, $B_0 + \Delta B = 534$G, and $a_{\rm gb} = -1405 a_0$.

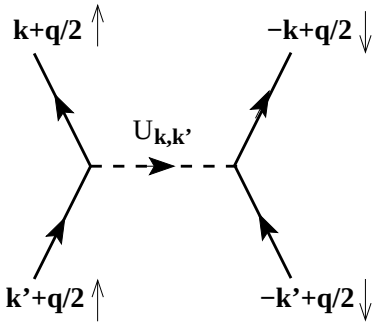

Figure 2.6: Scattering described by the Hamiltonian (2.9).

atoms weakly attract each other and, as we explained in Sec. 1.3 can undergo a BCS transition to a superfluid phase of loosely bound (and strongly overlapping) Cooper pairs. In contrast, when $a < 0$ and $1/k_F|a| \gg 1$, pairs of atoms are tightly bound in (composite) bosonic molecules which can undergo usual Bose-Einstein condensation (see Fig. 2.5). The reason why this is a *crossover* rather than a transition is, as we will be explaining in Sec. 2.3.1, that at zero temperature both states can be described by the same ground state and that there is a smooth evolution between the two by varying the scattering length, $1/k_F a$. Note however that at finite temperatures, as we explained in Secs. 1.2.1 and 1.3, while in the BCS regime the temperature scale at which Cooper pairs form (see Eq. (1.24)) and condense (see Eq. (1.35)) are the same and are much lower than the degeneracy temperature ($\Delta_{\rm BCS} \sim k_B T_{\rm BCS} \ll k_B T_F$), in contrast in the BEC regime the critical temperature of condensation is of the same order of magnitude than the degeneracy temperature, $T_{\rm BEC} \sim T_F$, while $T_{\rm BEC}$ is much smaller than the dissociation temperature for the composite boson — i.e. molecules forms at much higher temperatures at which they condense.

2.3.1 Zero temperature: Variational approach

Let us consider a mixture of a Fermi gas atoms with mass m in two different hyperfine states, which we will indicate as the states $\uparrow$ and $\downarrow$, interacting via

a two-body potential $U(\mathbf{r})$ (see Fig. 2.6). We will see later that, in the case where the scattering length a is much larger than the range of the potential R_e, $|a| \gg R_e$, we can substitute the finite range potential with a contact potential (in order to do that we will need the renormalisation scheme (B.9) where the ultra-violet cut-off is given by $k_0 = 1/R_e$). For the moment being we will consider the general case, assuming that $k_F R_e \ll 1$, $|a| \gg R_e$. while the product $k_F a$ can be changed arbitrarily. The many-body Hamiltonian can be written as

$$\hat{H} = \sum_{\mathbf{k},\sigma=\uparrow,\downarrow} \epsilon_{\mathbf{k}} c^\dagger_{\mathbf{k}\sigma} c_{\mathbf{k}\sigma} + \frac{1}{V} \sum_{\mathbf{k},\mathbf{k}',\mathbf{q}} U_{\mathbf{k},\mathbf{k}'} c^\dagger_{\mathbf{k}+\mathbf{q}/2\uparrow} c^\dagger_{-\mathbf{k}+\mathbf{q}/2\downarrow} c_{-\mathbf{k}'+\mathbf{q}/2\downarrow} c_{\mathbf{k}'+\mathbf{q}/2\uparrow} \ , \quad (2.9)$$

where $\epsilon_{\mathbf{k}} = k^2/2m$. As in atomic gas experiments the number of atoms in the two states is fixed, it is convenient to work in the grand-canonical ensemble $\hat{H} - \mu\hat{N}$ introducing a chemical potential μ to fix the total number of particles

$$\hat{N} = \sum_{\mathbf{k},\sigma=\uparrow,\downarrow} c^\dagger_{\mathbf{k}\sigma} c_{\mathbf{k}\sigma} \ . \quad (2.10)$$

Note that we are assuming for the moment being that the mixture is prepared balancing the number of different species, $\hat{N}_\uparrow = \hat{N}_\downarrow$. In this case therefore the chemical potential of both species can be chosen to be equal. It is the subject of the third lecture (chapter 3) to understand what happens if we consider an unbalanced (or polarised) two-component Fermi mixture.

Problem: Show that, as proposed by Leggett in [16], the ground state

$$|\psi\rangle = \prod_{\mathbf{k}} \left(\cos\theta_{\mathbf{k}} + \sin\theta_{\mathbf{k}} c^\dagger_{\mathbf{k}\uparrow} c^\dagger_{-\mathbf{k}\downarrow} \right) |0\rangle \ , \quad (2.11)$$

where $\theta_{\mathbf{k}} = \theta_{-\mathbf{k}}$, interpolates between a BEC condensate of tightly bound molecules (when $1/k_F a \to +\infty$) to a BCS state (when $1/k_F a \to -\infty$).

Answer: If we introduce the composite operator

$$b^\dagger_{\mathbf{q}} = \sum_{\mathbf{k}} \varphi_{\mathbf{k}} c^\dagger_{\mathbf{k}+\mathbf{q}/2\uparrow} c^\dagger_{-\mathbf{k}+\mathbf{q}/2\downarrow} \ ,$$

then, defining $\varphi_{\mathbf{k}} = \tan\theta_{\mathbf{k}}$, we can rewrite the state (2.11) as

$$|\psi\rangle \propto \prod_{\mathbf{k}} e^{\varphi_{\mathbf{k}} c^\dagger_{\mathbf{k}\uparrow} c^\dagger_{-\mathbf{k}\downarrow}} |0\rangle = e^{b^\dagger_{\mathbf{q}=0}} |0\rangle \ .$$

This state is a coherent state describing the condensation of the composite bosonic particles $b^\dagger_{\mathbf{q}}$ in the ground state $\mathbf{q} = 0$. Note that this a good description for BEC only at zero temperature, while at finite temperature, the inclusion of thermal fluctuations for pairs (i.e., finite values of $\mathbf{q}$) is essential (see Sec. 2.3.3).

We want to use the ground state (2.11) as a variational ground state and minimised the expectation value $\langle\psi|\hat{H} - \mu\hat{N}|\psi\rangle$ using $\theta_{\mathbf{k}}$ as a variational parameter.

Problem: By introducing the order parameter

$$\Delta_{\mathbf{k}} \equiv= -\frac{1}{V}\sum_{\mathbf{k}'} U_{\mathbf{k},\mathbf{k}'}\langle\psi|c_{-\mathbf{k}'\downarrow}c_{\mathbf{k}'\uparrow}|\psi\rangle = -\frac{1}{2V}\sum_{\mathbf{k}'} U_{\mathbf{k},\mathbf{k}'}\sin 2\theta_{\mathbf{k}'} \ , \qquad (2.12)$$

show that gap equation $\partial\langle\psi|\hat{H}-\mu\hat{N}|\psi\rangle/\partial\theta_{\mathbf{k}} = 0$ and the averaged density of particles in the ground state $n = \langle\psi|\hat{N})|\psi\rangle/V$ are respectively given by:

$$\Delta_{\mathbf{k}} = -\frac{1}{V}\sum_{\mathbf{k}'} U_{\mathbf{k},\mathbf{k}'}\frac{\Delta_{\mathbf{k}'}}{2E_{\mathbf{k}'}} \qquad (2.13)$$

$$n = \frac{1}{V}\sum_{\mathbf{k}}\left(1-\frac{\xi_{\mathbf{k}}}{E_{\mathbf{k}}}\right) \ , \qquad (2.14)$$

where $E_{\mathbf{k}} = \sqrt{\xi_{\mathbf{k}}^2+\Delta_{\mathbf{k}}^2}$ is the quasi-particle spectrum and $\xi_{\mathbf{k}} = \epsilon_{\mathbf{k}} - \mu$.

Answer: One can easily evaluate

$$\langle\psi|\hat{H}-\mu\hat{N}|\psi\rangle = 2\sum_{\mathbf{k}}\xi_{\mathbf{k}}\sin^2\theta_{\mathbf{k}} + \frac{1}{4V}\sum_{\mathbf{k},\mathbf{k}'} U_{\mathbf{k},\mathbf{k}'}\sin 2\theta_{\mathbf{k}}\sin 2\theta_{\mathbf{k}'} \ ,$$

from which the minimisation w.r.t. $\theta_{\mathbf{k}}$ gives $\xi_{\mathbf{k}}\tan 2\theta_{\mathbf{k}} = \Delta_{\mathbf{k}}$, where the order parameter is defined in (2.12). From here one has that $\sin 2\theta_{\mathbf{k}} = \Delta_{\mathbf{k}}/E_{\mathbf{k}}$, therefore obtaining Eq. (2.13). As the number equation (2.14) is concerned, one can easily show that $\langle\psi|\hat{N}|\psi\rangle = 2\sum_{\mathbf{k}}\sin^2\theta_{\mathbf{k}}$.

Gap (2.13) and number (2.14) equations have to solved simultaneously in order to find the order parameter and the chemical potential. Note that, as already discussed in Sec. 1.3, on the BCS side of the resonance the density of particles is fixed by the value of the Fermi momentum (see Eq. (1.17)) and therefore $\mu \simeq \varepsilon_F$. In contrast, on the extreme BEC side we will see that $\mu < 0$ and its value is determined by the molecular binding energy, $\mu \simeq \epsilon_b/2$, which, in the universal regime, is given by the expression (2.7). Therefore we expect that while in the BCS limit the number of particles equation is used to derive the chemical potential, while the gap equation can be used to find the order parameter, in contrast, in the BEC limit, the gap equation can be used to fix the chemical potential, while the number equation can be used to find the order parameter.

Problem: Knowing that in the BEC limit one can use the approximation $\theta_{\mathbf{k}} \ll 1$ (see Fig. 2.7: going towards the BEC regime, the bound pairs become more and more tightly bound and therefore the distribution $n_{\mathbf{k}}$ becomes broader, as fermions with large $\mathbf{k}$ participate in the bound state formation), show that the gap equation (2.13) reduces to the Schrödinger equation for a single bound pair with energy given by:

$$\mu = \frac{\epsilon_b}{2} = -\frac{1}{2ma^2} \ . \qquad (2.15)$$

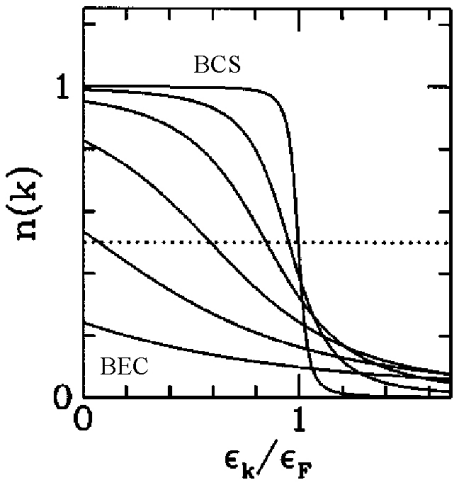

Figure 2.7: Number of particles at a given momentum $\mathbf{k}$, $n_{\mathbf{k}} = \sin^2\theta_{\mathbf{k}}$ versus $\epsilon_{\mathbf{k}}/\varepsilon_F$ across the BEC-BCS crossover (from [9]).

Answer: Note that, when $\theta_{\mathbf{k}} \ll 1$, $|\varphi_{\mathbf{k}}|^2 \simeq \theta_{\mathbf{k}}^2 \simeq n_{\mathbf{k}}$ and therefore $\theta_{\mathbf{k}}$ is the molecular wave-function. On this basis we already expect that $\theta_{\mathbf{k}}$ has to satisfy a Schrödinger equation describing a bound state with energy (2.7), $\epsilon_b = -1/ma^2$. In fact the gap equation reduces to $\Delta_{\mathbf{k}} \simeq 2\xi_{\mathbf{k}}\theta_{\mathbf{k}}$ and, from the definition of the order parameter (2.12), $\Delta_{\mathbf{k}} \simeq -(1/V)\sum_{\mathbf{k}'} U_{\mathbf{k},\mathbf{k}'}\theta_{\mathbf{k}'}$, we can write the equation satisfied by $\theta_{\mathbf{k}}$:

$$2\epsilon_{\mathbf{k}}\theta_{\mathbf{k}} + \frac{1}{V}\sum_{\mathbf{k}'} U_{\mathbf{k},\mathbf{k}'}\theta_{\mathbf{k}'} = 2\mu\theta_{\mathbf{k}} \ .$$

As $2\epsilon_{\mathbf{k}} = k^2/m$ is the kinetic energy of a molecule of mass $2m$, the gap equation becomes the Schrödinger equation for a single bound pair with binding energy $2\mu = \epsilon_b$. In the limit where the scattering length is much larger than than the range of the potential R_e (universal regime), $a \gg R_e$, we will explicitly show (for a contact potential) that $\epsilon_b = -1/ma^2$ (see Sec. 2.3.2).

2.3.2 Contact interaction

In the case of a contact interaction potential

$$U(\mathbf{r}) = g\delta(\mathbf{r}) \qquad\qquad U(\mathbf{k}) = g \ , \tag{2.16}$$

it is possible to obtain analytical results for the equations (2.13) and (2.14) in the extreme BCS and BEC limits (note that in this case the order parameter can be assumed to be uniform, $\Delta_{\mathbf{k}} = \Delta$). Note however that, as discussed in some detail in Sec. B.1.1, the contact interaction needs a renormalisation scheme towards ultra-violet (UV) divergences; it is easy to see that otherwise the gap equation diverges logarithmically. While in superconductors such a cut-off is represented by the Deby frequency ω_D, in atomic gases is represented by the

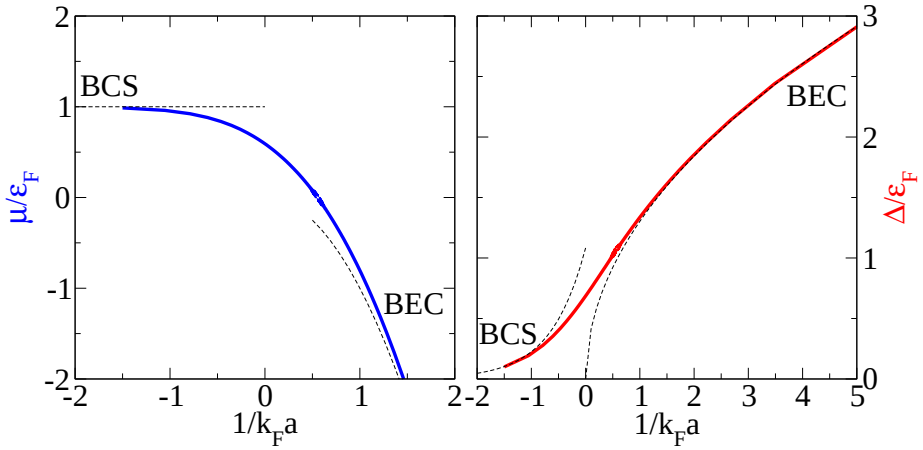

Figure 2.8: Chemical potential μ/ε_F (left) and order parameter Δ/ε_F (right) versus the scattering length $1/k_F a$ obtained by solving simultaneously the gap (2.18) and number (2.14) equations for a contact potential (2.16). The BCS and BEC asymptotic limits (dotted lines) have been explicitly derived in the Problem at page 24.

inverse range of the potential $k_0 = 1/R_e$. At the same time, one can introduce the scattering length via the expression (see Sec. B.1.1 and Eq. (B.9)):

$$\frac{m}{4\pi a} = \frac{1}{g} + \frac{1}{V}\sum_{\mathbf{k}}^{k_0} \frac{1}{2\epsilon_{\mathbf{k}}} \,. \tag{2.17}$$

In this way the logarithmic divergence of the gap equation is now cured,

$$\frac{m}{4\pi a} = \frac{1}{V}\sum_{\mathbf{k}}^{k_0} \left(\frac{1}{2\epsilon_{\mathbf{k}}} - \frac{1}{2E_{\mathbf{k}}} \right) \,, \tag{2.18}$$

and, when $ak_0 = a/R_e \gg 1$, the UV cut-off $k_0 = 1/R_e$ can be send to infinity, the dependence on the range of the scattering potential is lost and one is left with the dependence on the scattering length only (*universal regime*). Note that most of the current experiments are in this regime (*wide Feshbach resonances*), while for *narrow Feshbach resonances* one can show that the scattering length alone in not enough to describe the crossover but one also need the range of the potential — or alternatively two other parameters such as the detuning and the width of the resonance.

Problem: Show that in the BCS limit $1/k_F a \to -\infty$ ($\Delta \ll \varepsilon_F \simeq \mu$) the gap equation can be solved to give

$$\Delta = \frac{8}{e^2}\varepsilon_F e^{-\pi/2|a|k_F} \,, \tag{2.19}$$

while in the BEC limit $1/k_F a \to +\infty$ ($\varepsilon_F \ll \Delta \ll |\mu|$) one reobtains from (2.18) the energy of the molecular bound state (2.15).

Answer: It is useful to introduce the DoS per unit volume at the Fermi surface (see Eqs. (1.11) and (1.17))

$$\mathcal{N}(\varepsilon_F) = \frac{1}{V}N(\varepsilon_F) = \frac{m^{3/2}\sqrt{\varepsilon_F}}{\sqrt{2}\pi^2} = \frac{3}{4}\frac{n}{\varepsilon_F} \,, \tag{2.20}$$

in terms of which the scattering length reads $m/4\pi a = (\pi/2)\mathcal{N}(\varepsilon_F)/k_F a$. [a] Introducing the dimensionless units of energy, $x = \epsilon/|\mu|$, [b] one can write the gap equation in the form:

$$\frac{\pi}{2k_F a}\mathcal{N}(\varepsilon_F) = \mathcal{N}(|\mu|)\int_0^\infty dx\sqrt{x}\left[\frac{1}{2x} - \frac{1}{2\sqrt{(x\mp 1)^2 + (\Delta/|\mu|)^2}}\right] \,,$$

where the sign $\mp$ corresponds respectively to the cases $\mu >< 0$.
In the BCS limit, we know from the number equation (2.14) that, as $\Delta \ll \varepsilon_F$ (weak coupling regime), the chemical potential μ differs from the Fermi energy ε_F by an amount $O(\Delta^2/\varepsilon_F^2)$, $\mu \simeq \varepsilon_F$. Therefore the gap equation now reads

$$\frac{\pi}{2k_F a} = \underbrace{\int_0^\infty dx\sqrt{x}\left[\frac{1}{2x} - \frac{1}{2\sqrt{(x-1)^2 + (\Delta/\varepsilon_F)^2}}\right]}_{\ln(e^2\Delta/8\varepsilon_F)} \,,$$

from which one gets the expression (2.19).
In the BEC limit instead $\mu < 0$ and we have seen that $\theta_{\mathbf{k}} \simeq \Delta/2\xi_{\mathbf{k}} \ll 1$ (density of particles in the state $\mathbf{k}$), therefore in the first approximation we have that:

$$\frac{\pi}{2k_F a}\mathcal{N}(\varepsilon_F) \simeq \mathcal{N}(|\mu|)\underbrace{\int_0^\infty dx\sqrt{x}\left[\frac{1}{2x} - \frac{1}{2(x+1)}\right]}_{\pi/2} \,,$$

from which we get that $\sqrt{|\mu|/\varepsilon_F} = 1/k_F a$ and therefore Eq. (2.15). One can double-check that the energy scales are arranged as $\varepsilon_F \ll \Delta \ll |\mu|$ by solving the number equation in this limit

$$n \simeq \frac{\mathcal{N}(|\mu|)\Delta^2}{2|\mu|}\underbrace{\int_0^\infty dx\frac{\sqrt{x}}{(x+1)^2}}_{\pi/2} \,,$$

which gives $\Delta \simeq \sqrt{16/3\pi}\varepsilon_F\sqrt{1/k_F a}$. [c]

[a] Note that for a single component Fermi gas $\mathcal{N}(\varepsilon_F) = 3n/2\varepsilon_F$.

[b] One has:

$$\frac{1}{V}\sum_{\mathbf{k}} = \int\frac{d\mathbf{k}}{(2\pi)^3} = \int_0^\infty d\epsilon\mathcal{N}(\epsilon) \,.$$

[c] One can show that expanding to the next order

$$\left(\frac{\Delta}{\varepsilon_F}\right)^2 \simeq \frac{16}{3\pi}\frac{1}{k_F a} + \frac{4}{3\pi^2}(k_F a)^2 \,.$$

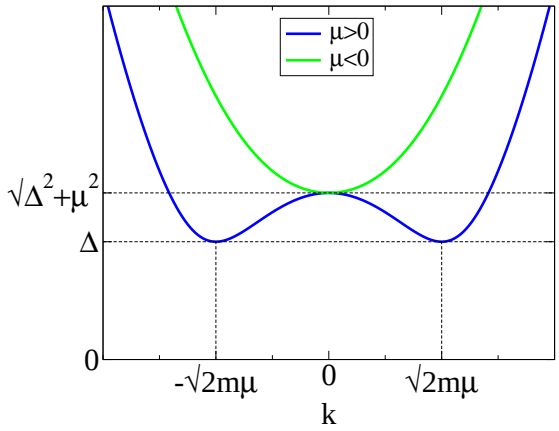

Figure 2.9: Quasi-particle excitation spectrum versus momentum on the BCS ($\mu > 0$) and on the BEC ($\mu < 0$) side of the resonance. The spectrum changes qualitatively from one shape to the other when $\mu = 0$.

The general behaviour of the chemical potential μ and the order parameter Δ obtained from solving simultaneously gap and number equations across the resonance is plotted in Fig. 2.8. The chemical potential is positive in the BCS limit, negative in the BEC limit, and changes sign across the resonance. The point at which the chemical potential changes sign, $\mu = 0$ can be interpreted as the point at which the crossover takes place. In fact it is at this point that the excitation energy of a quasiparticle with momentum $\mathbf{k}$, $E_{\mathbf{k}} = \sqrt{\xi_{\mathbf{k}}^2 + \Delta^2}$, changes qualitatively (see Fig. 2.9). In particular the gap of the excitation spectrum is given respectively by

$$E_{\rm gap} \equiv \min_{\mathbf{k}} E_{\mathbf{k}} = \begin{cases} \Delta & \mu > 0 \\ \sqrt{\Delta^2 + \mu^2} & \mu < 0 \, . \end{cases} \tag{2.21}$$

Note that $\mu = 0$ occurs on the molecular side of the resonance, i.e. for positive values of the scattering length, $1/k_F a \simeq 0.6$ (see Fig. 2.8), when already a molecular bound state exists.

2.3.3 Finite temperature

We have seen in the previous section that, at zero temperature, nothing particularly dramatic happens across the BEC-BCS crossover at the many body level, even when the scattering length goes through infinity at the resonance, while at the two-body level a molecular state appears or disappears. This is because at zero temperature, the very same BCS ground state (2.11) describes both BEC and BCS condensation regimes of respectively molecules and Cooper pairs [16].

At finite temperatures the situation is very different. This is because, at finite temperatures, the nature of condensation in the BCS and BEC limits is very different. In the BCS regime the formation and condensation of Cooper pairs occur at the same temperature or energy scale (e.g., $\Delta_{\rm BCS} \sim k_B T_{\rm BCS} \ll \varepsilon_F$). In this regime we have seen that the coupling is weak and the critical temperature depends exponentially on the interaction strength (or on the scattering

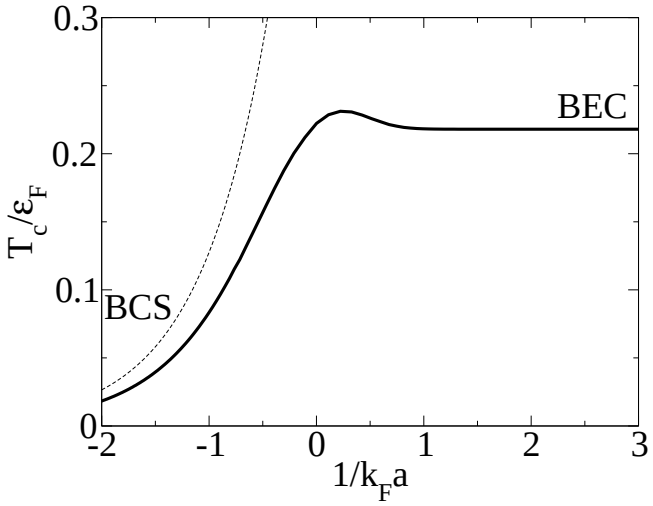

Figure 2.10: Critical temperature across the Feshbach resonance evaluated within the NSR approximation scheme [21]. The dashed line is the critical temperature in the BCS limit (see, e.g., (1.35)).

length). In contrast, in the BEC limit, the dissociation of molecules happens at temperatures much higher then the one at which the molecules condense ($T_{\rm BEC} \sim T_F \ll T_{\rm diss}$) — i.e., the condensate forms out of preformed molecules.

In more technical terms this means that, at finite temperatures, the mean-field description (introduced in Sec. 1.3 and also used previously in Sec. 2.3.1 across the entire crossover) cannot be a valid description any longer the closer we get towards the BEC regime. The mean-field approximation is only able to describe the pairing and un-pairing mechanism and, while it would give a good asymptotic description of the critical temperature in the BCS limit (see dashed line in Fig. 2.10), towards the BEC limit instead a mean-field description is only able to describe the dissociation temperature of the molecules (roughly proportional to the molecular binding energy), while molecules form well before they are able to condense. In order to take this into account one has to go beyond mean-field and at least, when fixing the number of particles as in Eq. (2.10), take into account the thermal (molecular) pairs.

As originally proposed by Nozières and Schmitt-Rink (NSR) [21], at the first approximation one has to add fluctuations above mean-field at the Gaussian level. Unfortunately there is no time during these lectures to go into any of these details. A review references to this method is given, e.g., by the Refs. [28, 32]. As an aside remark, note that even though the NSR approximation scheme gives a smooth crossover a finite temperature, as shown in Fig. 2.10, in the unitarity regime, where the scattering length is very large, not only mean-field is not a good approximation, but adding fluctuations corrections at one, two, and so on loops it is not a well controlled approximation; it is therefore questionable whether adding fluctuations at one loop order can give an answer for T_c quantitatively correct. This is a very interesting problem given that experiments are in fact close around this regime.

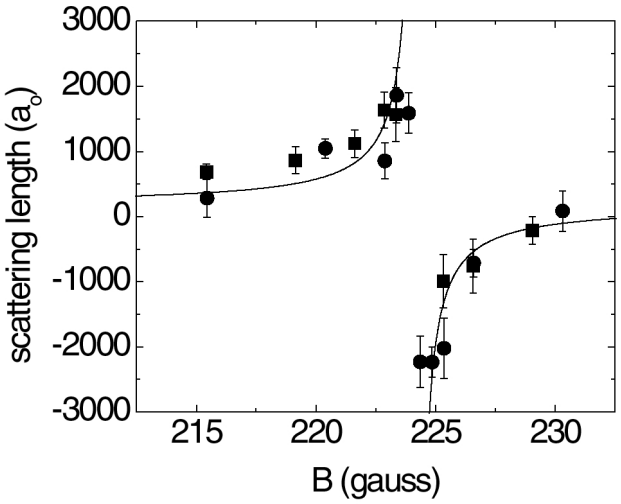

Figure 2.11: Scattering length measured for a Feshbach resonance at $B_0 \simeq 224.2$G ($a_{\rm bg} = 174a_0$ and $\Delta B \simeq 9.7$G) in a 50% mixture of states $|9/2, -9/2\rangle$ and $|9/2, -5/2\rangle$ in ^{40}K (from [30]).

2.4 Experiments on the BEC-BCS crossover

The main idea and results of the pioneering experiments on the BEC-BCS crossover for two-component Fermi mixtures with a Feshbach resonance will be discussed to some extent during the lectures. For reference to relevant papers see the captions of Figs. 2.11, 2.12, and 2.13.

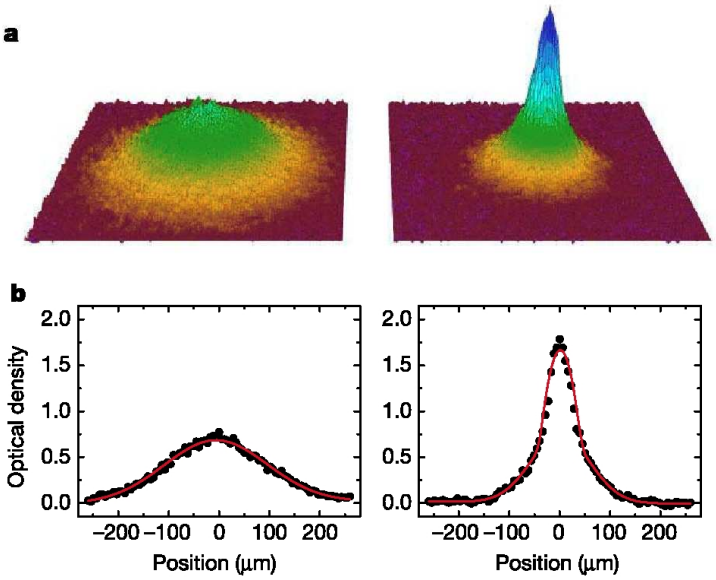

Figure 2.12: BEC of molecules in 50% mixture of states $|9/2, -9/2\rangle$ and $|9/2, -7/2\rangle$ in ^{40}K ($B_0 \simeq 202.2$G, $\Delta B \simeq 7.8$G) (from [10] and also see Refs. [29, 31]).

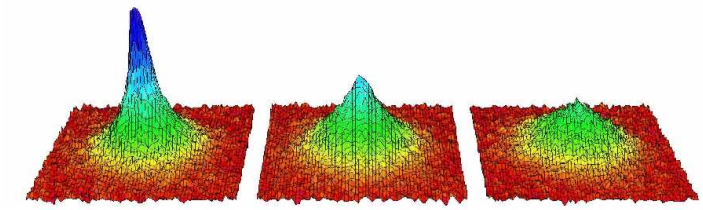

Figure 2.13: Condensation of fermionic pairs in ^{40}K (from [30]).

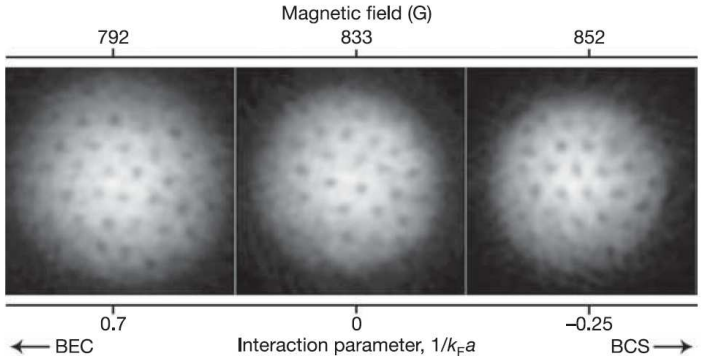

Figure 2.14: Observation of a vortex lattice in a strongly interacting rotating Fermi gas of ^{6}Li across a Feshbach resonance (from [39]).

Chapter 3

Lecture III: Polarised Fermi gases

We have seen in the previous two lectures that in experiments on ultracold gases it has been reached an unprecedented ability to control the interaction strength between the atoms via the Feshbach resonance mechanism. This has opened the possibility to study the phase diagram of various systems in very different regimes of interaction strength. In particular, in the case of two-component Fermi mixtures, Feshbach resonances have allowed to explore the crossover between a BEC phase of tightly bound molecules and a superfluid phase of loosely bound (Cooper) pairs, reminiscent of the Bardeen-Cooper-Schrieffer theory originally formulated for superconductors.

At the same time, in experiments is possible to achieve a full control over the number of atoms in their different spin species. In particular, the full control over the polarisation of a two-component Fermi mixture opens one of the most intriguing questions about the superfluid behaviour in fermionic systems: I.e., whether superfluidity can persist in presence of a population imbalance (or *polarisation*), when not every fermion can pair up (see Fig. 3.1).

This problem is highly relevant in different areas of physics, such as quantum chromodynamics (and compact stars), magnetised superconductors, electron-

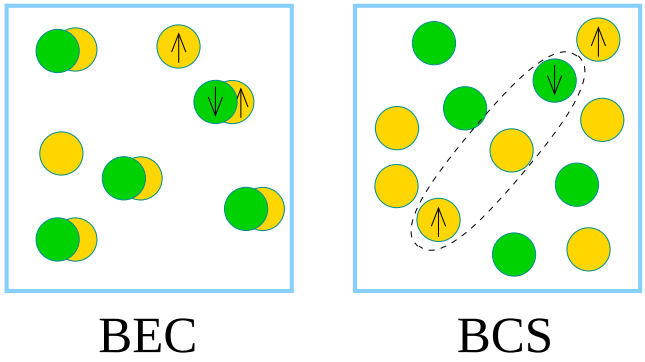

Figure 3.1: BEC-BCS crossover for imbalaced two-component Fermi gases with majority specie given by the atoms in the spin state $\uparrow$.

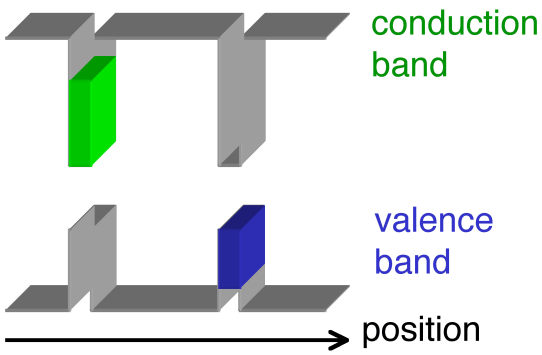

Figure 3.2: Schematic representation of electron-hole bilayers.

hole bilayers. In superconductors, though, the magnetic field used to generate spin imbalance via the Zeeman effect, also couples to the orbital degrees of freedom and as a result the magnetic field is expelled from the bulk of the superconductor (Meissner effect). We will briefly see in Sec. 3.1 how one can in principle engineer particular film geometries where the Zeeman effect is the dominant effect. In QCD, cold dense quark matter might form a colour superconductor – which might be relevant for describing neutron stars. The differences among the quark masses cause a mismatch among the Fermi surfaces between the species which pair. In electron-hole bilayers (see Fig. 3.2) it is possible to engineer semiconductor heterostructures with two quantum wells and to electrostatically (but also optically) load electrons in the conduction band of one well and holes in the valence band of the other well. The independent load by gating and biasing of the different wells, allows to create an imbalance in the populations of electrons and holes. As an aside comments about electron-hole bilayers, it is interesting to note that the idea of the BEC-BCS crossover has originated in the context of excitonic physics much earlier than even T. Leggett proposed it in his seminal paper [16]. The idea, due to a seminal work of Keldysh and Kopaev in 1965 [14], is that by increasing the density of electrons and holes, it is possible to explore the crossover between a low density (BEC) regime of tightly bound exciton pairs (i.e., hydrogenic atoms formed by one electron and one hole) and a high density regime where instead electrons and holes strongly overlap (and weakly attract each other) and can undergo a BCS-like transition to a state called exciton insulator (for a review see, e.g., Refs. [13, 17]). Atomic gases clearly provide an ideal testing ground for the quest of superfluidity in imbalanced Fermi systems, as the populations in two hyperfine states of the fermionic atoms can be easily controlled externally.

Our starting point will be the same Hamiltonian considered in Sec. 2.3.1 for two atoms in two spin-states, $\uparrow$ and $\downarrow$, interacting via a contact potential,

$$\hat{H} = \sum_{\mathbf{k},\sigma=\uparrow,\downarrow} \epsilon_{\mathbf{k}} c^{\dagger}_{\mathbf{k}\sigma} c_{\mathbf{k}\sigma} + \frac{g}{V} \sum_{\mathbf{k},\mathbf{k}',\mathbf{q}} c^{\dagger}_{\mathbf{k}+\mathbf{q}/2\uparrow} c^{\dagger}_{-\mathbf{k}+\mathbf{q}/2\downarrow} c_{-\mathbf{k}'+\mathbf{q}/2\downarrow} c_{\mathbf{k}'+\mathbf{q}/2\uparrow} \,, \tag{3.1}$$

where now however we allow for the density of particles in the two states,

$$\hat{n}_{\uparrow} = \frac{1}{V} \sum_{\mathbf{k}} c^{\dagger}_{\mathbf{k}\uparrow} c_{\mathbf{k}\uparrow} \qquad\qquad \hat{n}_{\downarrow} = \frac{1}{V} \sum_{\mathbf{k}} c^{\dagger}_{\mathbf{k}\downarrow} c_{\mathbf{k}\downarrow} \,,$$

to vary independently. Therefore, in order to do that, we have to introduce two different chemical potentials for each spin state, $\mu_\uparrow$ and $\mu_\downarrow$, or alternatively the averaged chemical potential μ and the 'Zeeman' term h (see Fig. 3.3 for the BCS limit):

$$\mu = \frac{\mu_\uparrow + \mu_\downarrow}{2} \qquad\qquad h = \frac{\mu_\uparrow - \mu_\downarrow}{2} \ . \tag{3.2}$$

At zero temperature, one can follow the same variational approach used in Sec. 2.3.1, minimising the expectation value $\langle\psi|\hat{H} - \mu\hat{n}V - h\hat{m}V|\psi\rangle$, where $\hat{n}$ and $\hat{m}$ are respectively the total density and the *population imbalance* (or *magnetisation*):

$$\hat{n} = \hat{n}_\uparrow + \hat{n}_\downarrow \qquad\qquad \hat{m} = \hat{n}_\uparrow - \hat{n}_\downarrow \ . \tag{3.3}$$

Note that we expect the ground state $|\psi\rangle$ to be the same whether an imbalance is present or not. In fact, introducing the order parameter as in Eq. (1.27), the Hamiltonian (3.1) in the mean-field approximation reads:

$$\hat{H} - \sum_{\sigma=\uparrow,\downarrow} \mu_\sigma \hat{n}_\sigma V \simeq \sum_{\mathbf{k}} \begin{pmatrix} c^\dagger_{\mathbf{k}\uparrow} & c_{-\mathbf{k}\downarrow} \end{pmatrix} \begin{pmatrix} \xi_{\mathbf{k}} - h & -\Delta \\ -\Delta & -\xi_{\mathbf{k}} - h \end{pmatrix} \begin{pmatrix} c_{\mathbf{k}\uparrow} \\ c^\dagger_{-\mathbf{k}\downarrow} \end{pmatrix} + \sum_{\mathbf{k}} (\xi_{\mathbf{k}} + h) - \frac{\Delta^2}{g} V \ , \tag{3.4}$$

where we are considering the case of the same specie (two-component) gas, i.e., equal masses $m_\uparrow = m_\downarrow = m$. [1] As the Zeeman term provides a rigid shift in energy and it does not change the symmetry of the Hamiltonian, it is clear that (3.4) can be diagonalised by the same unitary transformation considered in (1.29) in terms of the Bogoliubov operators $\gamma_{\mathbf{k},\sigma}$ (exercise),

$$\hat{H} - \sum_{\sigma=\uparrow,\downarrow} \mu_\sigma \hat{n}_\sigma V \simeq \sum_{\mathbf{k},\sigma=\uparrow,\downarrow} E_{\mathbf{k}\sigma} \gamma^\dagger_{\mathbf{k}\sigma} \gamma_{\mathbf{k}\sigma} + \sum_{\mathbf{k}} (\xi_{\mathbf{k}} - E_{\mathbf{k}}) - \frac{\Delta^2}{g} V \ ,$$

where now the quasi-particle energy is given by

$$E_{\mathbf{k}\sigma} = E_{\mathbf{k}} \mp h \ . \tag{3.5}$$

Therefore the ground state $|\psi\rangle$ has the same form as in (1.27) and corresponds to have a paired BCS-like state for all the values of $\mathbf{k}$ such that $E_{\mathbf{k}\downarrow} > 0$, while those $\mathbf{k}$ for which $E_{\mathbf{k}\downarrow} < 0$ are filled with only (non interacting) fermionic $\uparrow$ particles (majority species) and instead are depleted of $\downarrow$ particles (minority species). [2] In other words the free energy potential reads:

$$f(\Delta; h, \mu) \equiv \langle\psi|\hat{H} - \sum_{\sigma=\uparrow,\downarrow} \mu_\sigma \hat{n}_\sigma V|\psi\rangle = \sum_{\mathbf{k},\sigma=\uparrow,\downarrow} \Theta(-E_{\mathbf{k}\sigma}) E_{\mathbf{k}\sigma} + \sum_{\mathbf{k}} (\xi_{\mathbf{k}} - E_{\mathbf{k}}) - \frac{\Delta^2}{g} V \ . \tag{3.6}$$

[1] Note that mixing fermionic atoms of different species and therefore considering $m_\uparrow \neq m_\downarrow$ (such as ^{6}Li and and ^{40}K) can also create a mismatch of the Fermi surfaces in the BCS limit. Unequal masses mixtures will be not discussed here; for recent theoretical work see, e.g., Ref. [24] and references therein.

[2] Note that h can be fixed positive and that there is a symmetry for changing $h \mapsto -h$, which is equivalent to change the sign of the magnetisation, $m \mapsto -m$.

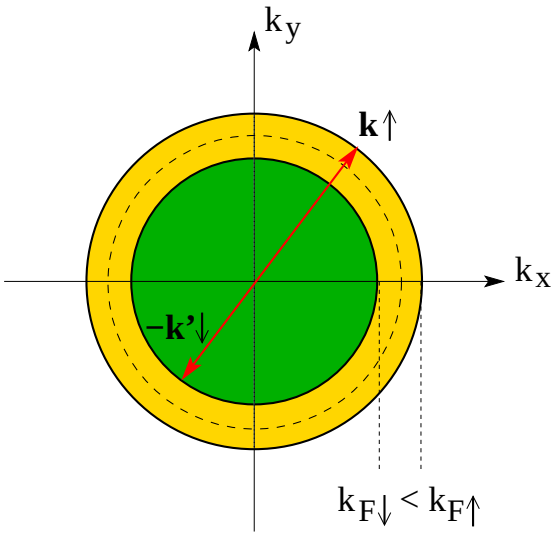

Figure 3.3: The imbalance between the density of atoms in the internal state $\uparrow$ and in the state $\downarrow$ determines, in the BCS limit, a mismatch of the two Fermi surfaces. The very same happens in a magnetised superconductor, when a Zeeman term causes a mismatch between the Fermi surface of spin $\uparrow$ electrons and the one of spin $\downarrow$ electrons.

As we are going to discuss in Sec. 3.2, a correct solution of this problem requires not only to solve simultaneously the gap equation, $\partial f(\Delta; h, \mu)/\partial\Delta = 0$, together with the number equations, as we instead did for the balanced BEC-BCS crossover problem in Sec. 2.3.1. In fact, we will see that the presence of a Zeeman term opens the possibility for first order transitions (and phase separation) and therefore the correct solution requires a proper minimisation of the free energy potential $f(\Delta; h, \mu)$ w.r.t. the order parameter Δ.

3.1 Analogy with magnetised superconductors

In the BCS limit ($\mu \simeq \varepsilon_F$) and at zero temperature, a two-component imbalanced problem admits an analytical solution. In this limit, the problem is equivalent with the one of a superconductor in presence of a Zeeman term, and it has been studied first by Sarma in 1963 [33].

For a superconductor in a thin-film geometry, it is possible to design a regime where the Zeeman effect dominates over the orbital effect. If the film thickness d is smaller than the penetration depth, the in-plane magnetic field lines enter the superconductor. Because of the orbital effect, the value of the critical magnetic field at which superconductivity is destroyed can be estimated by the condition that the magnetic flux associated to an area ξd (where ξ is the coherence length), is of the order of one flux quantum, $\phi_0 = hc/2e$, i.e. $H_c \xi d \sim \phi_0$. On the other hand, the critical field associated to the Zeeman splitting is obtained from the condition that the exchange energy splitting $h_Z \equiv g_L \mu_B H_Z$ (g_L is the Landé g-factor and $\mu_B = e/2m$ is the Bohr magneton) is of the size of the order parameter, $h_Z \sim \Delta$. Therefore, the orbital effect can be neglected when

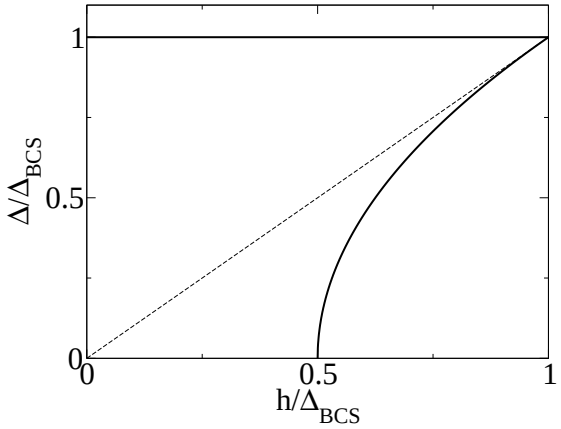

Figure 3.4: Two branches of the gap equation solution for the magnetised superconductor at zero temperature.

$H_Z < H_c$. I.e., when the thickness is smaller than a critical value, $d < d_c$, the dominant effect in suppressing superconductivity is the Zeeman splitting and the orbital effect can be neglected.

Problem: Show that for a magnetised superconductor (with attractive coupling constant $g \equiv -\lambda < 0$), the gap equation reads

$$\Delta = \lambda \mathcal{N}(\varepsilon_F) \int_{\sqrt{\max\{0, h^2-\Delta^2\}}}^{\omega_D} \frac{d\xi}{2\sqrt{\xi^2+\Delta^2}} \,, \tag{3.7}$$

(i.e., if $h > \Delta$ the quasi-particle states are occupied only for $\xi > \sqrt{h^2-\Delta^2}$) and that admits the following solution:

$$\Delta = \Delta_{\rm BCS} \begin{cases} 1 & h < \Delta \\ \sqrt{2h - \Delta_{\rm BCS}} \equiv \Delta_{\rm Sarma} & h > \Delta \,. \end{cases} \tag{3.8}$$

where $\Delta_{\rm BCS}$ is the BCS solution (1.31) (see Fig. 3.4) (**Hint:** Starting from the expression (3.6), consider the gap equation, $\partial f/\partial \Delta = 0$ and then use the BCS result (1.31) for $\Delta_{\rm BCS}$).

Therefore, at zero temperature and for $\Delta_{\rm BCS}/2 < h < \Delta_{\rm BCS}$, the gap equation for a magnetised superconductor admits three solution, $\Delta = 0$, $\Delta_{\rm BCS}$ and $\Delta_{\rm Sarma}$. The branch solution for $h > \Delta$ takes also the name of *Sarma state* [33]. However, by plotting the free energy potential $f(\Delta; h)$ as a function of Δ (see Fig. 3.5), one can easily see that the appearance of the Sarma state for $h \geq \Delta_{\rm BCS}/2$ correspond to a maximum of the free energy potential rather than a minimum, while $\Delta = 0$ is the real minimum energy solution. Therefore the study of the gap equation is not enough to know the phases of the system and one has to properly minimise the free energy. At zero temperature it turns

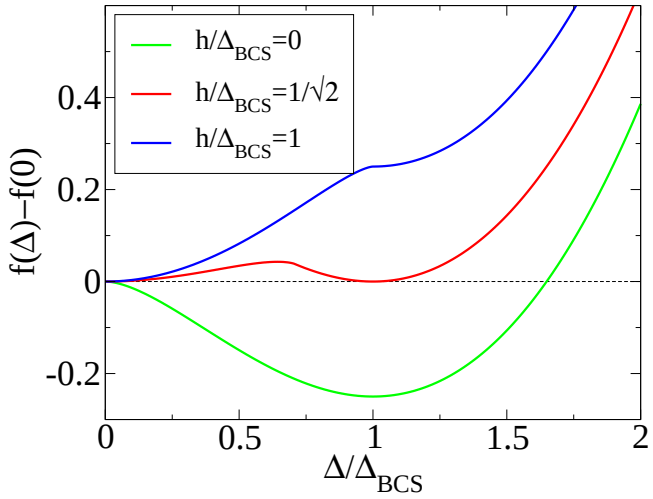

Figure 3.5: Free energy potential $f(\Delta, h)$ (rescaled by $f(0)$) versus the order parameter $\Delta/\Delta_{\rm BCS}$ for three different values of the rescaled Zeeman term $h/\Delta_{\rm BCS}$. When $h/\Delta_{\rm BCS} = 1/\sqrt{2}$ the system undergoes a first order phase transition where normal ($\Delta = 0$) and superconducting state ($\Delta = \Delta_{\rm BCS}$) coexist: I.e., for this value of the Zeeman term the system undergoes phase separation.

out that one can integrate exactly (3.6) (in the BCS limit) to get (exercise)

$$\frac{f(\Delta,h)-f(0)}{N(\epsilon_F)} = \Theta(\Delta-h)\left[\frac{\Delta^2}{2}\ln\left(\frac{\Delta}{\Delta_{\rm BCS}}\right)+\frac{2h^2-\Delta^2}{4}\right] + \Theta(h-\Delta)\left[\frac{\Delta^2}{2}\ln\left(\frac{h+\sqrt{h^2-\Delta^2}}{\Delta_{\rm BCS}}\right)-\frac{\Delta^2}{4}+\frac{h^2}{2}-\frac{h}{2}\sqrt{h^2-\Delta^2}\right] .$$

From its minimisation, we obtain that, when $h/\Delta_{\rm BCS} = 1/\sqrt{2}$, the system undergoes a first order phase transition from the superconducting phase ($\Delta = \Delta_{\rm BCS}$) to the normal phase ($\Delta = 0$). The fact the at $h/\Delta_{\rm BCS} = 1/\sqrt{2}$ the two phases have the same energy it means the system undergoes *phase separation* between the two phases.

At finite temperature, we can use the same argument used at the end of Sec. 1.3 to get the finite temperature free energy:

$$f(\Delta;h,\mu) = -\frac{\Delta^2}{g}+\frac{1}{V}\sum_{\mathbf{k}}\left[\xi_{\mathbf{k}}-E_{\mathbf{k}}-\frac{1}{\beta}\sum_{\sigma}\ln\left(1+e^{-\beta E_{\mathbf{k}\sigma}}\right)\right] , \qquad (3.9)$$

where the quasi-particle energy $E_{\mathbf{k}\sigma}$ has been defined in (3.5). Again the problem is particularly easy to solve in the BCS-limit. For $h = 0$ we already know that there is a second order phase transition between the superfluid (BCS) phase and the normal phase (one can show that $T_{\rm BCS} \simeq 0.57\Delta_{\rm BCS}$). In contrast for zero temperature we know that the transition is first order when $h = \Delta_{\rm BCS} = 1/\sqrt{2}$. Therefore we expect that the full phase diagram will have a *tricritical point* where the transition changes from 1$^{\rm st}$ to 2$^{\rm nd}$ (see Fig. 3.6). This problem was studied by Sarma [33].

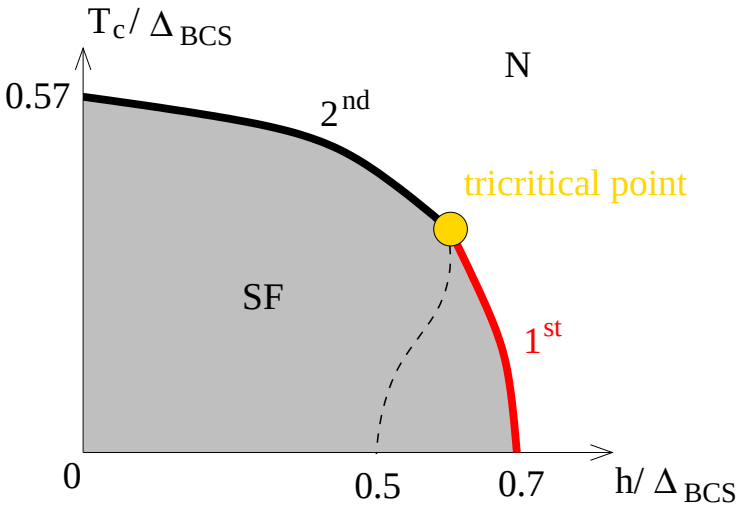

Figure 3.6: Finite temperature phase diagram for a polarised gas in the BCS limit (see Ref. [33] for the numerical result).

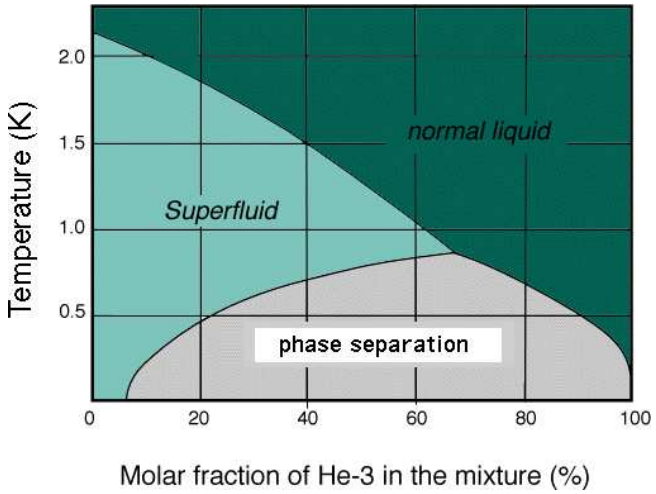

Figure 3.7: Phase diagram for the ^{3}He-^{4}He mixture: Critical temperature for the ^{4}He superfluid transition versus the fraction of ^{3}He in the mixture.

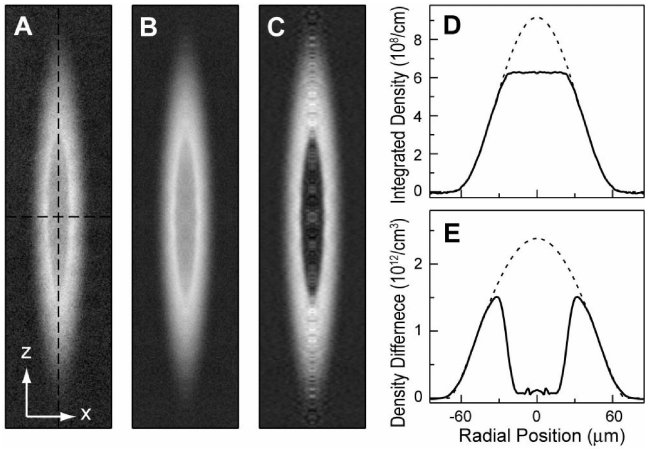

Figure 3.8: In-situ imaging of phase separation for an imbalanced two-component Fermi mixture in ^{6}Li at unitarity (from [35]).

3.2 Phase diagram across the resonance

The problem of polarised Fermi gases across the resonance is expected to be particularly rich. First of all let us notice a strong analogy between this problem and the one of ^{3}He-^{4}He mixtures — after all, in the extreme BEC regime, where all molecules are tightly bound, the polarised gas is a Bose-Fermi mixture. In ^{3}He-^{4}He mixtures, for small concentration of ^{3}He, the critical temperature (λ point) decreases with the concentration simply because one is effectively depleting the ^{4}He concentration — e.g., if ^{4}He would behave as an ideal Bose gas, one would have $T_c(x) = T_{\rm BEC}(1-x)^{2/3}$, where x is the molar fraction of ^{3}He in the mixture. However, for temperatures below the triple point (which corresponds to a tricritical point), the mixture phase separates into two liquid phases (similarly to how oil and water phase separates!).

We will discuss during the lecture (in general and qualitative terms) how this scenario is recovered in polarised gas Fermi gases and the topology of the phase diagram across the resonance (see Refs. [23, 24]).

3.3 Experiments on polarised Fermi gases

Experiments on two-component polarised Fermi gases are very recent (and in part work in progress) and represent one of the forefront experiments in the field of atomic gases. The main idea and results of the pioneering experiments in two-component polarised Fermi mixtures with a Feshbach resonance will be discussed to some extent during the lecture. For reference to relevant papers see the captions of Figs. 3.8 and 3.9.

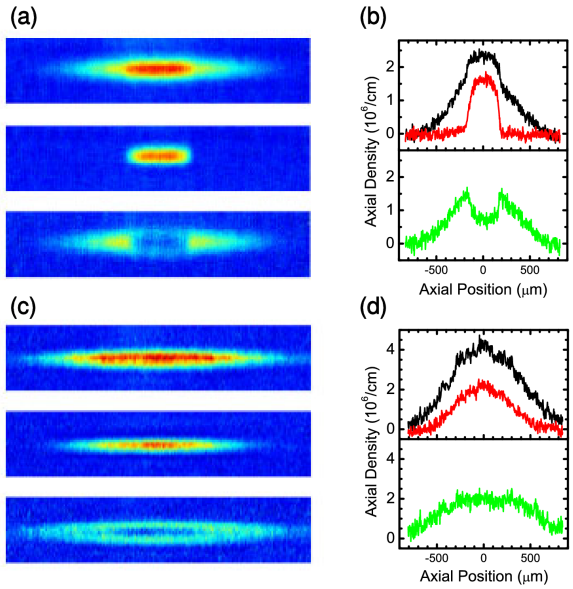

Figure 3.9: Temperature dependence of the transition to a phase separated state for an imbalanced two-component Fermi mixture in ^{6}Li at unitarity (from [25]): temperature is below the tricritical point in the upper frames (a) and (b) (where the transition is 1st order and there is phase separation), while temperature is above the tricritical point in the lower frames (c) and (d) (where the transition is 2nd order.

Appendix A

Alkali atoms

The properties of atomic structure of alkali atoms are important for the experimental study of ultracold atomic gases. We discuss here the basic elements.

A.1 Hyperfine levels and Zeeman splitting

In alkali atoms all electrons but one occupy closed shells and therefore have a single valence electron in an s orbital. Therefore the alkali atom electronic spin is $S = J = 1/2$ (and the orbital angular momentum in the ground state is zero, $L = 0$). The value of the alkali atom nuclear spin I depends instead on the isotopic species. Moreover, as their atomic number Z is odd (and neutral atoms have an equal numbers of electrons and protons), alkali atoms with odd mass number $A = Z + N$ (even number of neutrons N) are **bosons**, while those with even mass number A (odd N) are **fermions** (see Table A.1).

The nuclear spin $\hat{\mathbf{I}}$ is coupled to the electronic angular momentum $\hat{\mathbf{J}} = \hat{\mathbf{L}} + \hat{\mathbf{S}}$ by the hyperfine interaction

$$\hat{H}_{\rm hf} = A\hat{\mathbf{I}} \cdot \hat{\mathbf{J}} \,, \tag{A.1}$$

where $A \propto \mu$ is a constant proportional to the magnetic moment of the nucleus μ (note that for all alkali atoms listed in Table A.1 except ^{40}K $\mu > 0$). The eigenstates of $\hat{H}_{\rm hf}$ are given by the eigenstates $|F, m_F\rangle$ of total angular momentum

$$\hat{\mathbf{F}} = \hat{\mathbf{I}} + \hat{\mathbf{J}} \,, \tag{A.2}$$

bosons	^{1}H	N=0	I=1/2	$\mu > 0$
	^{85}Rb	N=48	I=5/2	$\mu > 0$
	^{87}Rb	N=50	I=3/2	$\mu > 0$
	^{23}Na	N=12	I=3/2	$\mu > 0$
	^{7}Li	N=4	I=3/2	$\mu > 0$
fermions	^{6}Li	N=3	I=1	$\mu > 0$
	^{40}K	N=21	I=4	$\mu < 0$

Table A.1: Alkali atoms used in experiments with their neutron number N, nuclear spin I and nuclear magnetic moment μ.

as $2\hat{\mathbf{I}}\cdot\hat{\mathbf{J}} = \hat{\mathbf{F}}^2 - \hat{\mathbf{I}}^2 - \hat{\mathbf{J}}^2$ ($\hat{\mathbf{F}}^2|F,m_F\rangle = F(F+1)|F,m_F\rangle$ and $\hat{F}_z|F,m_F\rangle = m_F|F,m_F\rangle$). For alkali atoms $S = J = 1/2$ and therefore $F = I \pm 1/2$ ($m_F = m_I + m_S$ is instead degenerate), giving the two hyperfine energy levels

$$E_{F=I+1/2} = \frac{A}{2}I \qquad\qquad E_{F=I-1/2} = -\frac{A}{2}(I+1)\ ,$$

and the hyperfine splitting

$$\Delta E_{\rm hf} = A\left(I+\frac{1}{2}\right)\ . \tag{A.3}$$

Characteristic frequencies of the hyperfine splitting are in the range $\Delta E_{\rm hf} \simeq 1 - 10$GHz.

Magnetic trapping of alkali atoms exploits the Zeeman effect on the atomic energy levels:

$$\hat{H} = A\hat{\mathbf{I}}\cdot\hat{\mathbf{S}} + CS_z\ , \tag{A.4}$$

where $C = 2\mu_B B$ ($\mu_B = |e|/2m_e$ is the Bohr magneton) and where we have neglected the Zeeman effect on the nuclear spin, DI_z, as $D/C \sim m_e/m_p \sim 1/2000$. In the weak magnetic field limit, when the Zeeman energies are small compared with the hyperfine splitting, one case use perturbation theory to evaluate the matrix element

$$\langle F,m_F|\hat{S}_z|F,m_F\rangle = \frac{m_F}{2}\frac{S(S+1)+F(F+1)-I(I+1)}{F(F+1)}\ ,$$

where, we have made use of the relations $[\hat{\mathbf{F}}^2,[\hat{\mathbf{F}}^2,\hat{S}_z]] = 2(\hat{\mathbf{F}}^2\hat{S}_z + \hat{S}_z\hat{\mathbf{F}}^2) - (\hat{\mathbf{S}}\cdot\hat{\mathbf{F}})\hat{F}_z$ and $\hat{\mathbf{I}}^2 = \hat{\mathbf{S}}^2 + \hat{\mathbf{F}}^2 - 2\hat{\mathbf{S}}\cdot\hat{\mathbf{F}}$, therefore getting the following approximated expression for the atomic energy levels:

$$\begin{aligned} E_{F,m_F} &\simeq \frac{A}{2}\left[F(F+1) - I(I+1) - S(S+1)\right] + g_L\mu_B m_F B \\ g_L &= \frac{S(S+1)+F(F+1)-I(I+1)}{F(F+1)}\ , \end{aligned} \tag{A.5}$$

where g_L is the Landé factor. Many experiments are carried out at relatively low magnetic fields, where (A.5) apply.

However, for a general value of the magnetic field B, either $\hat{\mathbf{F}}^2$ nor $\hat{\mathbf{S}}^2, \hat{S}_z, \hat{\mathbf{I}}^2, \hat{I}_z$ are good quantum numbers any longer, but *only* $\hat{F}_z$ *is conserved* ($m_F = m_I \pm 1/2$). As $m_F = m_I \pm 1/2$, one can reduce the total Hamiltonian $\hat{H}$ in 2×2 subspaces with fixed m_F. The eigenvalues of (A.4) have to be determined by diagonalisation: By using the relation $\hat{\mathbf{I}}\cdot\hat{\mathbf{S}} = I_zS_z + (I_+S_- + I_-S_+)/2$, one can construct the matrix elements of (A.4) on the basis $|m_I,m_S\rangle$, where $-I \le m_I \le I$ and $m_S = \pm 1/2$. The energy levels obtained by such diagonalisation will be labelled by F and m_F (where F indicates only where the eigenvalues comes from for $B = 0$).

A.1.1 The I=3/2 example (^{87}Rb, ^{23}Na, ^{7}Li)

Let's consider for example the case of $I = 3/2$, valid for atoms like ^{87}Rb, ^{23}Na and ^{7}Li. For the states with $m_F = \pm 2$ (also called *doubly polarised states*) one

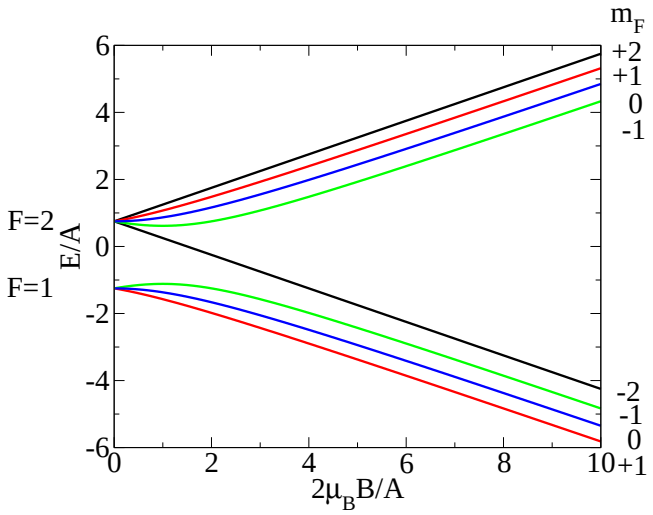

Figure A.1: Hyperfine energy levels for $I = 3/2$.

can only have

$$|F=2, m_F=2\rangle = |m_I = \frac{3}{2}, m_S = \frac{1}{2}\rangle \qquad E_{m_F=2} = \frac{3}{4}A + \frac{C}{2}$$
$$|F=2, m_F=-2\rangle = |m_I = -\frac{3}{2}, m_S = -\frac{1}{2}\rangle \qquad E_{m_F=-2} = \frac{3}{4}A - \frac{C}{2}\ .$$

For $m_F = 1$ instead one has to diagonalise (A.4) on the subspace of $|m_I = 3/2, m_S = -1/2\rangle$ and $|m_I = 1/2, m_S = 1/2\rangle$,

$$\begin{pmatrix} -3A/4 - C/2 & \sqrt{3}A/2 \\ \sqrt{3}A/2 & A/4 + C/2 \end{pmatrix}$$

which eigenvalues we will indicate with

$$|F=2, m_F=1\rangle = \cos\theta |m_I = \frac{3}{2}, m_S = -\frac{1}{2}\rangle + \sin\theta |m_I = \frac{1}{2}, m_S = -\frac{1}{2}\rangle$$
$$|F=1, m_F=1\rangle = -\sin\theta |m_I = \frac{3}{2}, m_S = -\frac{1}{2}\rangle + \cos\theta |m_I = \frac{1}{2}, m_S = -\frac{1}{2}\rangle\ ,$$

according to their $B = 0$ value:

$$E_{m_F=1} = -\frac{A}{4} \pm \sqrt{\frac{3}{4}A^2 + \frac{1}{4}(A+C)^2}\ .$$

Analogously one can proceed for the $m_F = -1$ and the $m_F = 0$ states:

$$E_{m_F=-1} = -\frac{A}{4} \pm \sqrt{\frac{3}{4}A^2 + \frac{1}{4}(A-C)^2}$$
$$E_{m_F=1} = -\frac{A}{4} \pm \sqrt{A^2 + \frac{1}{4}C^2}\ .$$

The energy levels are plotted in Fig. A.1.

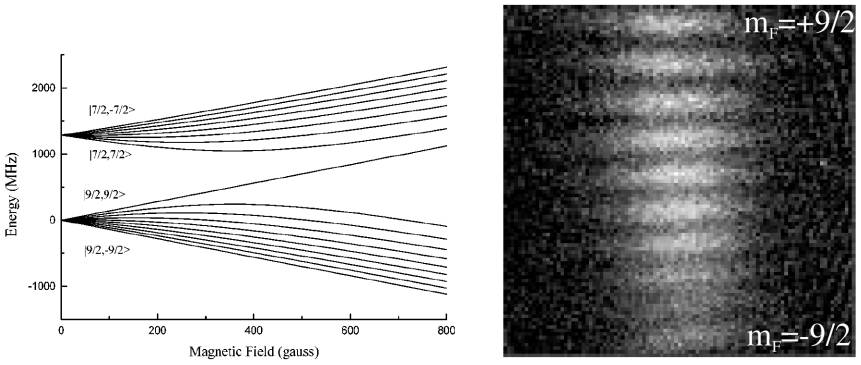

(a) (b)

Figure A.2: The different hyperfine states of ^{40}K (a) (from [5]) can be separated and imaged with a Stern-Gerlach field (b) (from [18]).

Aside the *doubly polarised states* ($F = I + 1/2$, $m_F = F$), the *maximally stretched state* ($F = I - 1/2$, $m_F = -(I - 1/2)$) plays an important role in experiments.

Problem: Evaluate the energy levels in ^{40}K.

Answer: The hyperfine energy levels are given by

$$E_{F=7/2} = \frac{5}{2}|A| \qquad\qquad E_{F=9/2} = -2|A| \,,$$

and therefore the hyperfine spitting is given by $\Delta E_{hf} = 9A/4$. Note that, because of the negative nuclear magnetic moment, $A < 0$, the $F = 9/2$ level has lower energy than the $F = 7/2$ one. In presence of an external magnetic field the energy level are plotted in Fig. A.2.

Appendix B

Elements of scattering theory

In this appendix we briefly (and roughly) explain how, given a certain scattering potential $U(\mathbf{r})$, it is possible to derive the s-wave scattering length a defined in (2.5). For a detailed description see, e.g., Refs. [7, 26].

A general solution of the scattering problem (2.2) can be expanded in the eigenstates of the angular momentum $\hat{\mathbf{L}}$, the Legendre polynomials $P_\ell(\cos\theta)$:

$$\psi_{\mathbf{k}}(\mathbf{r}) = \sum_{\ell=0}^{\infty} A_\ell P_\ell(\cos\theta) \frac{u_{k,\ell}(r)}{kr} \ . \tag{B.1}$$

Substituting into (2.2) it is easy to show that the radial wave-function $u_{k,\ell}(r)$ satisfies the equation

$$\frac{d^2 u_{k,\ell}(r)}{dr^2} + \left[k^2 - \frac{\ell(\ell+1)}{r^2} - 2m_r U(r) \right] u_{k,\ell}(r) = 0 \ . \tag{B.2}$$

The term $\ell(\ell+1)/r^2$ represents the centrifugal barrier for finite ℓ states (see Fig. B.1). Note that, for identical atoms (prepared in the same hyperfine state) the values of ℓ are restricted to even values for bosons and to odd values for fermions. Scattering for identical fermions prepared in the same hyperfine states in the p-wave ($\ell = 1$) channel is in general strongly suppressed at low temperatures — although can be revived via a Feshbach resonance and this is at the moment an active field of research.

At large distances one can neglect the centrifugal term and the scattering potential, therefore the radial wave-function has the form

$$u_{k,\ell}(r) \simeq \sin[kr - \frac{\pi\ell}{2} + \delta_\ell(k)] \ ,$$

where $\delta_\ell(k)$ are phase shifts. By considering the expansion of the plain wave e^{ikz} on Legendre polynomials, one can then show that scattering amplitude (2.3) and scattering cross section (2.4) can be expressed in terms of the phase shift

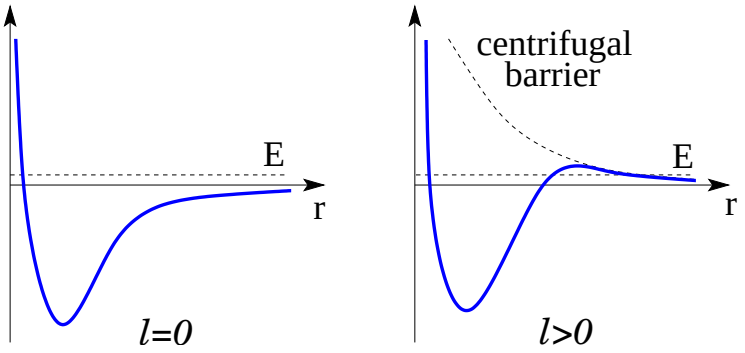

Figure B.1: Effective scattering potential $U(r)+\ell(\ell+1)/(2m_r r^2)$ for $\ell = 0$ (left) and $\ell \geq 1$ (right).

in the following way:

$$f(\theta) = \frac{1}{2ik}\sum_{\ell=0}^{\infty}(2\ell+1)[e^{2i\delta_\ell(k)}]P_\ell(\cos\theta)$$
$$\sigma = \frac{4\pi}{k^2}\sum_{\ell=0}^{\infty}(2\ell+1)\sin^2\delta_\ell(k)\ .$$

In order to find explicitly the phase shifts $\delta_\ell(k)$, one has to solve the Schrödinger equation (B.2). We are going to do it for the simple case of a *square potential well* for s-wave scattering ($\ell = 0$) only and refer to Ref. [7] for more general cases. In particular one can show that for a finite range potential one has that

$$\delta_\ell(k) \underset{k\to 0}{\sim} k^{2\ell+1}\ ,$$

and therefore the scattering cross section is dominated by the $\ell = 0$ (s=wave) term, for which the scattering amplitude $f_{\ell=0}(\theta) = \delta_0(k)/k$ and therefore, from (2.5),

$$a \equiv -\lim_{k\to 0}\frac{\delta_0(k)}{k}\ .$$

Equivalently, at low energy, one expects the following asymptotic behaviour for the radial wave-function:

$$\lim_{k\to 0} u_{k,\ell=0}(r) \propto r - a\ .$$

Problem: Determine the scattering length for a square potential well (see Fig. B.2).

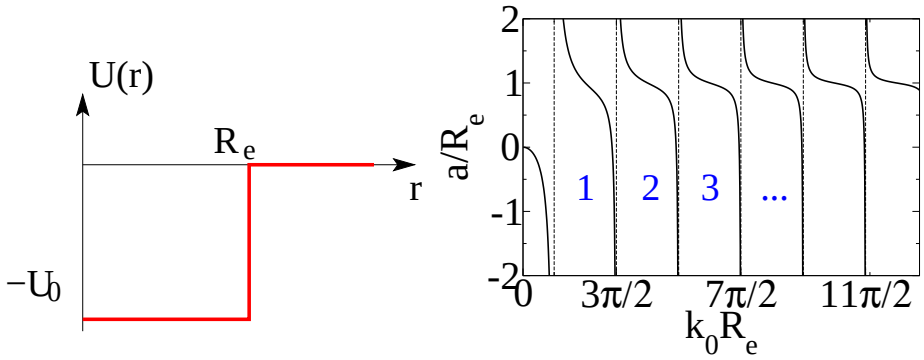

Figure B.2: Square potential well (left) and associated scattering length (right). The number of bound states which the potential can hold increases every time $k_0 R_e = (2n+1)\pi/2$.

Answer: We have to solve the Schrödinger equation for the radial wave function in the low energy ($k \to 0$) limit:

$$\frac{d^2u(r)}{dr^2} - 2m_r U(r)u(r) = 0 \, .$$

For the solution

$$u(r) = \begin{cases} c_1(r-a) & r > R_e \\ c_2 \sin(k_0 r) & r < R_e \, , \end{cases}$$

where $k_0 = \sqrt{2m_r U_0}$, we have to impose continuity of $u(r)$ and $du(r)/dr$ at $r = R_e$, obtaining the following expression for the scattering length (see Fig. B.2):

$$a = R_e - \frac{\tan(k_0 R_e)}{k_0} \, . \tag{B.3}$$

Therefore one has that when $k_0 R_e = \sqrt{2m_r U_0} R_e < \pi/2$, the depth of the potential well U_0 is too small to allocate a bound states and the scattering length is negative implying an *attractive* effective interaction between the atoms (see Eq. (2.6)). Increasing the value of U_0 eventually the well is deep enough to hold a bound state, at which point the scattering length becomes positive and the effective interaction between the atoms is *repulsive*. By increasing further the value of $k_0 R_e$ the sequence repeats and every time a new bound states is created the scattering length goes from $-\infty$ to $+\infty$ at $k_0 R_e = (2n+1)\pi/2$. The relation between the divergence of the scattering length and the appearance of a bound state is general. At the same time, when $k_0 R_e$ increases, the scattering length is more likely to be mainly positive.

B.1 T-matrix formalism

At low energies and large distances it is useful to define the scattering properties in terms of the T-matrix. This can be defined considering the scattering

problem (2.2) written in the momentum representation,

$$(\epsilon_{r\mathbf{k}} - \epsilon_{r\mathbf{k}'})\,\psi^{\rm sc}(\mathbf{k}') = U(\mathbf{k}-\mathbf{k}') + \int \frac{d\mathbf{k}''}{(2\pi)^3} U(\mathbf{k}'-\mathbf{k}'')\psi^{\rm sc}(\mathbf{k}'')\;, \tag{B.4}$$

where $\epsilon_{r\mathbf{k}} = k^2/2m_r$ and where, taking the Fourier transform of Eq. (2.3), $\psi(\mathbf{k}') = (2\pi)^3\delta(\mathbf{k}-\mathbf{k}') + \psi^{\rm sc}(\mathbf{k}')$ and $U(\mathbf{r}) = \int d\mathbf{k}/(2\pi)^3 e^{i\mathbf{k}\cdot\mathbf{r}}U(\mathbf{k})$. Therefore the scattered (outgoing) wave can be defined in terms of the scattering T-matrix as

$$\begin{aligned}\psi^{\rm sc}(\mathbf{k}') &= (\epsilon_{r\mathbf{k}} - \epsilon_{r\mathbf{k}'} + i\delta)^{-1}\,T(\mathbf{k}',\mathbf{k})\\ T(\mathbf{k}',\mathbf{k}) &\equiv U(\mathbf{k}-\mathbf{k}') + \int \frac{d\mathbf{k}''}{(2\pi)^3} U(\mathbf{k}'-\mathbf{k}'')\psi^{\rm sc}(\mathbf{k}'')\;.\end{aligned}$$

From its definition it follows that the T-matrix satisfies the following (self-consistency) Lippmann-Schwinger equation

$$\hat{T} = \hat{U} + \hat{U}\hat{G}_0\hat{T}\;, \tag{B.5}$$

where the free Green's function is given by

$$\hat{G}_0 = [(\epsilon_r + i\delta)\hat{\mathbb{I}} - \hat{H}_0]^{-1} \tag{B.6}$$

and where we have used a matrix notation. [1] One can formally write the solution of Eq. (B.5) as

$$\hat{T} = (\mathbb{I} - \hat{U}\hat{G}_0)^{-1}\hat{U} = \hat{U}(\mathbb{I} - \hat{G}_0\hat{U})^{-1}\;. \tag{B.7}$$

In the zero-energy limit, $E \to 0$ ($k \to 0$), and at large distances, one can express the scattering length defined in Eq. (2.5) in terms of the T-matrix. In fact in this limit one has that

$$\psi^{\rm sc}(\mathbf{k}') \simeq \frac{1}{-\epsilon_{r\mathbf{k}'} + i\delta} T(0,0)\;,$$

and therefore, considering the Fourier transform of this expression, [2] we obtain that

$$\psi^{\rm sc}_{\mathbf{k}}(\mathbf{r}) \underset{\mathbf{k}\to 0, r\to\infty}{\simeq} -\frac{2m_r}{4\pi r} T(0,0)\;,$$

and therefore, from (2.5), the scattering length:

$$a = \frac{2m_r}{4\pi} T(0,0)\;. \tag{B.8}$$

[1] I.e., we should read (B.5) as an operator equation in momentum space:

$$\langle\mathbf{k}'|\hat{T}|\mathbf{k}\rangle = \langle\mathbf{k}'|\hat{U}|\mathbf{k}\rangle + \langle\mathbf{k}'|\hat{U}\frac{1}{V}\sum_{\mathbf{k}''}|\mathbf{k}''\rangle\langle\mathbf{k}''|\hat{G}_0|\mathbf{k}''\rangle\langle\mathbf{k}''|\hat{T}|\mathbf{k}\rangle\;,$$

where $T(\mathbf{k},\mathbf{k}') = \langle\mathbf{k}'|\hat{T}|\mathbf{k}\rangle$, $U(\mathbf{k}-\mathbf{k}') = \langle\mathbf{k}'|\hat{U}|\mathbf{k}\rangle$, and where $\hat{G}_0$ is diagonal in momentum space, $G_0(\mathbf{k}) = (E + i\delta - \epsilon_{r\mathbf{k}})^{-1}$.

[2] I.e.

$$\int \frac{d\mathbf{k}'}{(2\pi)^3}\frac{e^{i\mathbf{k}'\cdot\mathbf{r}}}{k'^2} = \frac{1}{(2\pi)^2}\int_0^\infty dk' \underbrace{\int_{-1}^{1} d(\cos\theta) e^{ik'r\cos\theta}}_{\frac{2}{k'r}\sin(k'r)} = \frac{1}{2\pi^2 r}\underbrace{\int_0^\infty dx \frac{\sin x}{x}}_{\pi/2} = \frac{1}{4\pi r}\;.$$

Therefore $T(0,0)$ describes the low energy and large distances scattering properties of the scattering potential U and allow not to deal with the details of the interaction when two atoms are close to each other, but only with the asymptotic behaviour when they are far from each other. The Born approximation corresponds to consider the first term in the expansion in $\hat{U}$ in Eq. (B.7), $T(\mathbf{k},\mathbf{k}') \simeq U(\mathbf{k}-\mathbf{k}')$, and therefore we obtain the expression (2.6).

B.1.1 Contact interaction

An useful application of the T-matrix formalism is the renormalisation of the contact interaction coupling strength via the introduction of the scattering length, which we are using in Sec. 2.3.2. A contact interaction potential (2.16) is clearly ill-defined — e.g., Eq. (B.5) is ill-defined for a contact interaction. Also the gap-equation is divergent for a contact interaction and needs a cut-off. In the case of superconductivity the cut-off is provided by the Deby frequency ω_D (see, e.g., Eq. (1.22)). We will see here that for atomic gases we can send the ultraviolet (UV) cut-off to infinity by introducing the scattering length.

As every term of the expansion of the Lippmann-Schwinger equation (B.5) is ill-defined for a contact interaction potential (2.16), we introduce by hand an UV cut-off in momentum space k_0, which physically represents the *range of the interaction*, $k_0 = 1/R_e$. In this way we can write every term of the expansion as

$$T(0,0) = g\left[1+\sum_{n=1}^{\infty}\left(\frac{g}{V}\sum_{\mathbf{k}}^{k_0}\frac{1}{-\epsilon_{r\mathbf{k}}}\right)^n\right] = g\left[1-\frac{g}{V}\sum_{\mathbf{k}}^{k_0}\frac{1}{-\epsilon_{r\mathbf{k}}}\right]^{-1} .$$

By making use of the relation between the T-matrix and the scattering length a (B.8) we obtain the following renormalisation condition

$$\frac{2m_r}{4\pi a} = \frac{1}{g} + \frac{1}{V}\sum_{\mathbf{k}}^{k_0}\frac{1}{\epsilon_{r\mathbf{k}}} . \tag{B.9}$$

as shown in Sec. 2.3.2, this condition is enough to renormalise the gap equation, where, once a is introduced, the UV cut-off can be sent to infinity. For two atoms with equal masses m, $2m_r = m$ and $\epsilon_{r\mathbf{r}} = 2\epsilon_{\mathbf{k}}$, where $\epsilon_{\mathbf{k}} = k^2/2m$.

Appendix C

Elements of cooling and trapping techniques

In alkali atoms, with the exception of polarised hydrogen atoms, the pressure versus temperature phase transition line for BEC condensation falls into the region where the system at equilibrium is instead a solid (see Fig. C.1).

Problem: Evaluate the pressure-temperature phase transition line for a non-interacting Bose gas:

$$P = \zeta(5/2)\left(\frac{m}{2\pi}\right)^{3/2}(k_B T)^{5/2} \ . \tag{C.1}$$

Answer: The total energy of an ideal Bose gas for $T < T_{\rm BEC}$ ($\mu = 0$) is given by

$$E = \int_0^\infty d\epsilon N(\epsilon) f_B(\epsilon; \mu = 0) \ ,$$

where $f_B(\epsilon; \mu = 0) = (e^{\epsilon/k_B T} - 1)^{-1}$ and where the DoS $N(\epsilon)$ has been defined in (1.11). From $\int_0^\infty dx x^{\alpha-1}(e^x - 1)^{-1} \equiv \Gamma(\alpha)\zeta(\alpha)$ ($\Gamma(5/2) = 3\sqrt{\pi/2}/2$) and from the definition of pressure for a homogeneous gas in three-dimensions, $P = 2E/3V$, one obtains (C.1). Note that the expression of the pressure turns out to be independent from the volume of the gas, i.e. in a BEC phase of an ideal gas the compressibility of the gas is infinite. This pathology is modified by including interaction effects.

Therefore the BEC configuration is unstable as in thermal equilibrium the system should be in a crystal phase: The BEC phase in alkali gases can only exists as a *metastable phase*. This means that if the gas is diluted enough and the interaction between two atoms happens only via 2-*body collisions* (see Sec. 2.1 and the appendix B), then two particles that scatter on each other cannot form a (molecular) bound state. In fact, energy and momentum conservation require that only 3-*body collisions* allow the formation of molecules, the first step in the formation of a solid: Of the three atoms colliding, two form a molecule and the third one can carry away the residual energy. Therefore metastability means that the time-scale for molecule formation via 3-body collisions ($\sim n^3$) is longer than the time needed by the gas to reach kinetic equilibrium via 2-body

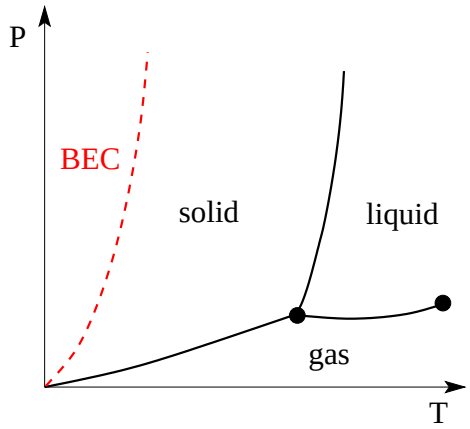

Figure C.1: Schematic pressure P vs. temperature T phase diagram for alkali atoms. The BEC phase transition line (red dashed) lies in the region where the equilibrium state is a solid.

scattering ($\sim n^2$): This gives a window at very low densities where metastability is possible and where the lifetime of the gas can be in a range between seconds and minutes. An exception is provided by a gas of polarised hydrogen atoms (i.e. hydrogen atoms with parallel electronic spin), as this is characterised by a strong repulsive interaction (see Fig. C.2). Spin-polarised hydrogen remains a gas down to zero temperature and BEC can here be realised in a true equilibrium state.

At the same time, the condition for BEC requires $\lambda_T > n^{-1/3}$ (see (1.1)), therefore *dilute atomic gases* have to be cooled down at *ultralow temperature*. Typical order of magnitudes for BEC are:

$$T \sim 500\text{nK} - \mu\text{K} \qquad\qquad n \sim 10^{13} - 10^{15}\text{cm}^{-3} \, .$$

In order to reach these conditions one needs sophisticated techniques of

1. *trapping the atoms* — the gas has to be kept away from any material wall, where interaction with other atoms would favour the formation of molecules;

2. *evaporative and laser cooling* — in order to reach such a ultracold temperatures.

Few basic elements and experimental examples of cooling and trapping techniques will be given during the course of the lectures. For an introductory review see, e.g., Refs. [26, 27].

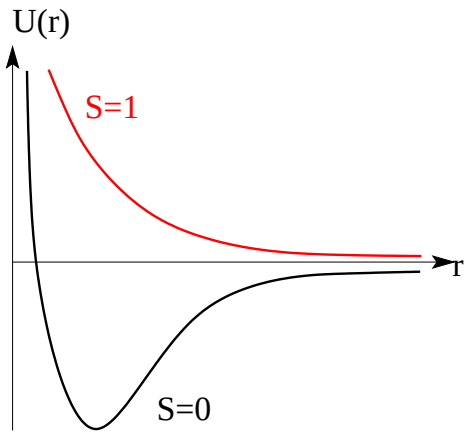

Figure C.2: Sketch of the singlet ($S = 0$) and triplet ($S = 1$) interaction potentials (see Sec. 2.1) for hydrogen atoms: While the triplet potential is always repulsive, the singlet one allows the formation of H_2 molecules.

Bibliography

[1] A. A. Abrikosov. *Fundamentals of the Theory of Metals.* Elsevier, 1988.

[2] M. H. Anderson, J. R. Ensher, M. R. Matthews, C. E. Wieman, and E. A. Cornell. Observation of bose-einstein condensation in a dilute atomic vapor. *Science*, 269:198, 1995.

[3] J. Bardeen, L. N. Cooper, and J. R. Schrieffer. Microscopic theory of superconductivity. *Phys. Rev.*, 106:162, 1957.

[4] I. Bloch, J. Dalibard, and W. Zwerger. Many body physics with ultracold gases. 2007.

[5] J. L. Bohn, J. P. Burke, C. H. Greene, H. Wang, P. L. Gould, and W. C. Stwalley. Collisional properties of ultracold potassium: Consequences for degenerate bose and fermi gases. *Phys. Rev. A*, 59(5):3660, 1999.

[6] L. N. Cooper. Bound electron pairs in a degenerate fermi gas. *Phys. Rev.*, 104(4):1189–1190, Nov 1956.

[7] J. Dalibard. Collisional dynamics of ultra-cold atomic gases. *Proceedings of the International School of Physics Enrico Fermi, Course CXL: Bose – Einstein condensation in gases*, 1998.

[8] K. B. Davis, M. O. Mewes, M. R. Andrews, N. J. van Druten, D. S. Durfee, D. M. Kurn, and W. Ketterle. Bose-einstein condensation in a gas of sodium atoms. *Phys. Rev. Lett.*, 75(22):3969, 1995.

[9] J. R. Engelbrecht, M. Randeria, and C. A. R. Sáde Melo. Bcs to bose crossover: Broken-symmetry state. *Phys. Rev. B*, 55(22):15153, 1997.

[10] M. Greiner, C. A. Regal, and D. S. Jin. Emergence of a molecular bose-einstein condensate from a fermi gas. *Nature*, 426:537, 2004.

[11] A. Griffin, D. Snoke, and S. Stringari, editors. *Bose-Einstein Condensation.* Cambridge University Press, Cambridge, 1995.

[12] D. S. Jin, B. De Marco, and S Papp. Exploring a quantum degenerate fermi gas. *ICAP proceedings*, 2000.

[13] L. V. Keldysh. Macroscopic coherent states of excitons in semiconductors. In Griffin et al. [11], page 246.

[14] L. V. Keldysh and Yu V. Kopaev. *Sov. Phys. Solid State*, 6:2219, 1965.

[15] T. Köhler, K. Góral, and P. S. Julienne. Production of cold molecules via magnetically tunable feshbach resonances. *Rev. Mod. Phys.*, 78(4), 2006.

[16] A. J. Leggett. Diatomic molecules and cooper pairs. *Modern Trends in the Theory of Condensed Matter*, 1980.

[17] P. B. Littlewood, P. R. Eastham, J. M. J. Keeling, F. M. Marchetti, B. D. Simons, and M. H. Szymanska. Models of coherent exciton condensation. *J. Phys.: Condens. Matter*, 16:S3597, 2004.

[18] T. Loftus, C. A. Regal, C. Ticknor, J. L. Bohn, and D. S. Jin. Resonant control of elastic collisions in an optically trapped fermi gas of atoms. *Phys. Rev. Lett.*, 88(17):173201, 2002.

[19] B. De Marco and D. S. Jin. Onset of fermi degeneracy in a trapped atomic gas. *Science*, 285:1703, 1999.

[20] G. Modugno. Fermi-bose mixture with tunable interactions. 2007.

[21] P. Nozières and S. Schmitt-Rink. Bose condensation in an attractive fermion gas; from weak to strong coupling superconductivity. *J. LTP*, 59(3):195, 1985.

[22] S. Ospelkaus, C. Ospelkaus, L. Humbert, K. Sengstock, and K. Bongs. Tuning of heteronuclear interactions in a degenerate fermi-bose mixture. *Phys. Rev. Lett.*, 97:120403, 2006.

[23] M. M. Parish, F. M. Marchetti, A. Lamacraft, and B. D. Simons. Finite temperature phase diagram of a polarised fermi condensate. *Nature Phys.*, 3:124, 2007.

[24] M. M. Parish, F. M. Marchetti, A. Lamacraft, and B. D. Simons. Polarized fermi condensates with unequal masses: Tuning the tricritical point. *Phys. Rev. Lett.*, 98:160402, 2007.

[25] G. B. Partridge, Wenhui Li, Y. A. Liao, R. G. Hulet, M. Haque, and H. T. C. Stoof. Deformation of a trapped fermi gas with unequal spin populations. *Phys. Rev. Lett.*, 97(19):190407, 2006.

[26] C. J. Pethick and H. Smith. *Bose-Einstein Condensation is Dilute Gases.* Cambridge University Press, Cambridge, 2002.

[27] Lev. P. Pitaevskii and Sandro Stringari. *Bose-Einstein Condensation.* Clarendon Press, Oxford, 2003.

[28] M. Randeria. Crossover from BCS theory to Bose-Einstein condensation. In Griffin et al. [11], page 355.

[29] C. A. Regal, M. Greiner, and D. S. Jin. Lifetime of molecule-atom mixtures near a feshbach resonance in k. *Phys. Rev. Lett.*, 92:083201, 2004.

[30] C. A. Regal and D. S. Jin. Measurement of positive and negative scattering lengths in a fermi gas of atoms. *Phys. Rev. Lett.*, 90:230404, 2003.

[31] C. A. Regal, C. Ticknor, J. L. Bohn, and D. S. Jin. Creation of ultracold molecules from a fermi gas of atoms. *Nature*, 424:47, 2003.

[32] C. A. R. Sá de Melo, M. Randeria, and J. R. Engelbrecht. Crossover from bcs to bose superconductivity: Transition temperature and time-dependent ginzburg-landau theory. *Phys. Rev. Lett.*, 71(19):3202, 1993.

[33] G. Sarma. *J. Phys. Chem. Solids*, 24:1029, 1963.

[34] J. R. Schrieffer. *Theory if Superconductivity.* Perseus Books, U.S., 1999.

[35] Y. Shin, M. W. Zwierlein, C. H. Schunck, A. Schirotzek, and W. Ketterle. Observation of phase separation in a strongly-interacting imbalanced fermi gas. *Phys. Rev. Lett.*, 97:030401, 2006.

[36] M. Tinkham. *Introduction to Superconductivity.* McGraw-Hill Education, 1995.

[37] A. G. Truscott, K. E. Strecker, W. I. McAlexander, G. B. Partridge, and R. G. Hulet. Observation of fermi pressure in a gas of trapped atoms. *Science*, 291:2570, 2001.

[38] M. Zaccanti, C. D'Errico, F. Ferlaino, G. Roati, M. Inguscio, and G. Modugno. Control of the interaction in a fermi-bose mixture. *Phys. Rev. A*, 74:041605, 2006.

[39] M.W. Zwierlein, J.R. Abo-Shaeer, A. Schirotzek, C.H. Schunck, and W. Ketterle. Vortices and superfluidity in a strongly interacting fermi gas. *Nature*, 435:1047, 2005.